7

Reflections on Magnetohydrodynamics

H. K. MOFFATT

1 Introduction

Magnetohydrodynamics (MHD) is concerned with the dynamics of fluids that are good conductors of electricity, and specifically with those effects that arise through the interaction of the motion of the fluid and any ambient magnetic field $\boldsymbol{B}(\boldsymbol{x}, t)$ that may be present. Such a field is produced by electric current sources which may be either external to the fluid (in which case we may talk of an 'applied' magnetic field), or induced within the fluid itself. The induction of a current distribution $\boldsymbol{j}(\boldsymbol{x}, t)$ by flow across the field $\boldsymbol{B}$ is the result of Faraday's 'law of induction'. The resulting Lorentz force distribution $\boldsymbol{F}(\boldsymbol{x}, t) = \boldsymbol{j} \wedge \boldsymbol{B}$ is generally rotational, i.e. $\nabla \wedge \boldsymbol{F} \neq 0$, and therefore generates vorticity in the fluid. There is thus a fundamental interaction between the velocity field $\boldsymbol{v}$ and the magnetic field $\boldsymbol{B}$, an interaction which not only leads to modification of well-understood flows of 'conventional' fluid dynamics, but also is responsible for completely new phenomena that simply do not exist in non-conducting fluids.

There are three major fields of application of magnetohydrodynamics, which will be discussed in this survey in the following order.

1.1 Liquid-metal magnetohydrodynamics

This is a branch of the subject which has attracted increasing attention over the last 30 years, and which has been much stimulated by the experimental programmes of such laboratories as MADYLAM in Grenoble, and the Laboratory of Magnetohydrodynamics in Riga, Latvia. These programmes have been motivated by the possibility of using electromagnetic fields in the processing of liquid metals (and their alloys) in conditions that frequently require high temperatures and high purity. These fields can be used to levitate samples of liquid metal, to control their shape, and to induce internal

stirring for the purpose of homogenization of the finished product, all these being effects that are completely unique to magnetohydrodynamics. Electromagnetic stirring (exploiting the rotationality of the Lorentz force) is used in the process of continuous casting of steel and other metals; and magnetic fields have an important potential use in controlling the interface instabilities that currently limit the efficiency of the industrial process of extracting aluminium from the raw material cryolite. The industrial exploitation of MHD in such contexts is of relatively recent origin, and great developments in this area are to be expected over the next few decades.

1.2 Magnetic fields in planetary physics and astrophysics

Nearly all large rotating cosmic bodies, which are either partly or wholly fluid in composition, exhibit magnetic fields of predominantly internal origin, i.e. fields associated with internal rather than external currents. Such fields may be generated by amplification of a very weak applied field, a process that may be limited by the conductivity of the fluid. More dramatically however, such fields may be the result of a 'dynamo instability' which is entirely of internal origin; this can occur (as in the liquid core of the Earth) if buoyancy-driven convection interacts with Coriolis forces to produce 'helicity' in the flow field. When the dynamo instability occurs, the field energy grows exponentially until the Lorentz forces are strong enough to modify the flow; at this stage, the magnetic energy is at least of the same order as the kinetic energy of the flow that generates it, and may even (as in the Earth context) be much greater. A fundamental understanding of this process in the context of turbulent flow has developed slowly over the last 50 years; and our present understanding of turbulent dynamo action, although incomplete, must surely be regarded as one of the great achievements of research in turbulence of this last half-century.

1.3 Magnetostatic equilibrium, structure and stability

This large area of MHD is also important in astrophysical contexts; but it has received even greater stimulus from the field of fusion physics and the need to design fusion reactors containing hot fully ionized gas (or plasma) isolated from the containing solid boundaries by a suitably engineered magnetic field – such an arrangement being conventionally described as a 'magnetic bottle'. In ideal circumstances, the gas in such a bottle is at rest, in equilibrium under the mutual action of Lorentz and pressure forces. Pressure forces of course tend to make the gas expand; the Lorentz force must thus be such as

to prevent this expansion. Moreover the equilibrium, if it is to be effective, must be stable: the energy of the system must be minimal with respect to variations associated with the vast family of perturbations available to such a system. It is this problem of stability, first recognized and analysed in the 1950s, which has bedevilled the subject ever since, and which still stands in the way of development of an energy-producing thermonuclear reactor. Progress has nevertheless been sustained, and there is still a degree of optimism that the full stability problem can be eventually, if not solved, at least sufficiently tamed to allow design of commercially viable reactors. This is truly one of the immense scientific challenges that continues to face mankind at the dawn of the new millennium. Its solution would provide a clean source of low-cost energy at least until the next reversal of the Earth's magnetic field; by then we may have other problems to worry about!

2 Fundamental principles

The electromagnetic field is governed by Maxwell's equations, and it is legitimate in all the above contexts to adopt the 'magnetohydrodynamic approximation' in which displacement current and all associated relativistic effects are neglected. The magnetic field is then related to current by Ampere's equation

$$\nabla \wedge \boldsymbol{B} = \mu_0 \boldsymbol{j} \qquad \text{with} \qquad \nabla \cdot \boldsymbol{B} = 0, \tag{2.1}$$

where μ_0 is constant ($4\pi \times 10^{-7}$ in SI units). Moreover $\boldsymbol{B}$ evolves according to Faraday's law of induction which may be expressed in the form

$$\partial \boldsymbol{B}/\partial t = -\nabla \wedge \boldsymbol{E}, \tag{2.2}$$

where $\boldsymbol{E}(\boldsymbol{x}, t)$ is the electric field in the 'laboratory' frame of reference. The current in this frame is related to $\boldsymbol{E}$ and $\boldsymbol{B}$ by Ohm's law:

$$\boldsymbol{j} = \sigma(\boldsymbol{E} + \boldsymbol{v} \wedge \boldsymbol{B}), \tag{2.3}$$

where $\boldsymbol{v}(\boldsymbol{x}, t)$ is the velocity field and σ is the electrical conductivity of the fluid. Like viscosity, σ is temperature dependent, and will therefore in general be a function of $\boldsymbol{x}$ and t in the fluid. We shall, however, neglect such variations, and treat σ as a given constant fluid property. Note that the field $\boldsymbol{E}' = \boldsymbol{E} + \boldsymbol{v} \wedge \boldsymbol{B}$ appearing in (2.3) is the electric field in a frame of reference moving with the local fluid velocity $\boldsymbol{v}$.

From the above equations, we have immediately

$$\frac{\partial \boldsymbol{B}}{\partial t} = \nabla \wedge (\boldsymbol{v} \wedge \boldsymbol{B}) + \eta \nabla^2 \boldsymbol{B}, \tag{2.4}$$

where $\eta = (\mu_0\sigma)^{-1}$, the 'magnetic diffusivity' (or 'resistivity') of the fluid. Equation (2.4) is the famous 'induction equation' of magnetohydrodynamics, describing the evolution of $\boldsymbol{B}$ if $\boldsymbol{v}(\boldsymbol{x},t)$ is known. The equation has a marvellous generality: it holds quite independently of the particular dynamical forces generating the flow (e.g. whether these are of thermal or compositional origin, whether the Lorentz force is or is not important, whether Coriolis forces are present or not); it holds also whether $\boldsymbol{v}$ is incompressible ($\nabla\cdot\boldsymbol{v} = 0$) or not. Equation (2.4) may be regarded as the vector analogue of the scalar advection–diffusion equation

$$\frac{\partial\theta}{\partial t} + \boldsymbol{v}\cdot\nabla\theta = \kappa\nabla^2\theta, \tag{2.5}$$

which describes the evolution of a scalar contaminant $\theta(\boldsymbol{x},t)$ subject to molecular diffusivity κ. Clearly, it is desirable to extract from (2.4) as much information as we can, before specializing to any particular dynamical context.

Note first the striking analogy, first pointed out by Batchelor (1950), between equation (2.4) and the equation for vorticity $\boldsymbol{\omega} = \nabla\wedge\boldsymbol{u}$ (the use of $\boldsymbol{u}$ rather than $\boldsymbol{v}$ here is deliberate) in a non-conducting barotropic fluid of kinematic viscosity ν:

$$\frac{\partial\boldsymbol{\omega}}{\partial t} = \nabla\wedge(\boldsymbol{u}\wedge\boldsymbol{\omega}) + \nu\nabla^2\boldsymbol{\omega}. \tag{2.6}$$

The analogy is incomplete in that $\boldsymbol{\omega}$ is constrained by the relationship $\boldsymbol{\omega} = \nabla\wedge\boldsymbol{u}$, whereas $\boldsymbol{B}$ and $\boldsymbol{v}$ in (2.4) suffer no such constraint: there is in effect far more freedom in (2.4) than there is in (2.6)! Nevertheless a number of results familiar in the context of (2.6) do carry over to the context of (2.4).

2.1 The magnetic Reynolds number

First, suppose that the system considered is characterized by a length scale l_0 and a velocity scale v_0. Naïve comparison of the two terms on the right of (2.4) gives

$$\frac{|\nabla\wedge(\boldsymbol{v}\wedge\boldsymbol{B})|}{|\eta\nabla^2\boldsymbol{B}|} \sim \frac{v_0 l_0}{\eta} = R_m, \tag{2.7}$$

the magnetic Reynolds number, defined by obvious analogy with the Reynolds number of classical fluid dynamics. The three major areas of application of magnetohydrodynamics specified in the introduction may be discriminated in terms of this single all-important dimensionless number:

(*a*) $R_m \ll 1$: this is the domain of liquid-metal magnetohydrodynamics in most (but not quite all) circumstances of potential practical importance. In this situation, diffusion dominates induction by fluid motion, and the magnetic field in the fluid is determined, at least at leading order, by geometrical considerations (the geometry of the fluid domain and of the external current-carrying coils or magnets). The additional field induced by the fluid motion is weak compared with the applied field.

(*b*) $R_m = O(1)$: this is the regime in which dynamo instability, analogous in some respects to the dynamical instabilities of a flow that may lead to turbulence, may occur. Such instability requires that, in some sense, induction represented by the term $\nabla \wedge (\boldsymbol{v} \wedge \boldsymbol{B})$ in (2.4) dominates the diffusion term $\eta \nabla^2 \boldsymbol{B}$, which tends to eliminate field in the absence of external sources. Thus dynamo instability may be expected to be associated with an instability criterion of the form

$$R_m > R_{mc}\,, \tag{2.8}$$

where R_{mc} is a critical magnetic Reynolds number, presumably of order unity; it must immediately be added that a condition such as (2.8) may be necessary but by no means sufficient for dynamo instability, which may require additional much more subtle conditions on the field $\boldsymbol{v}$.

(*c*) $R_m \gg 1$: here we are into the domain of 'nearly perfect conductivity', in which inductive effects dominate diffusion. The limit $R_m \to \infty$ (or $\sigma \to \infty$ or $\eta \to 0$) may be described as the perfect-conductivity limit. In this formal limit, $\boldsymbol{B}$ satisfies what is known as the 'frozen-field equation'

$$\frac{\partial \boldsymbol{B}}{\partial t} = \nabla \wedge (\boldsymbol{v} \wedge \boldsymbol{B})\,, \tag{2.9}$$

which implies that the flux Φ of $\boldsymbol{B}$ across any material (Lagrangian) surface S is conserved:

$$\frac{\mathrm{d}\Phi}{\mathrm{d}t} = 0 \qquad \text{where} \qquad \Phi = \int_S \boldsymbol{B} \cdot \boldsymbol{n}\, \mathrm{d}S\,. \tag{2.10}$$

This is Alfvén's theorem, the analogue of Kelvin's circulation theorem, and one of the results for which the incomplete analogy between (2.4) and (2.6) is reliable. The fact that, in the perfect-conductivity limit, magnetic lines of force are 'frozen in the fluid' provides an appealing picture of how a magnetic field may develop in time. By analogy with vorticity in an incompressible fluid, any motion that tends to stretch magnetic field lines (or '$\boldsymbol{B}$-lines' for short), will also tend to intensify magnetic field. Is this a manifestation of dynamo action? Sometimes it is, but by no means invariably, as we shall see.

2.2 Magnetic helicity conservation

Since $\nabla \cdot \boldsymbol{B} = 0$, we may always introduce a vector potential $\boldsymbol{A}(\boldsymbol{x}, t)$ with the properties

$$\boldsymbol{B} = \nabla \wedge \boldsymbol{A}, \qquad \nabla \cdot \boldsymbol{A} = 0. \tag{2.11}$$

The 'uncurled' version of (2.9) is then

$$\frac{\partial \boldsymbol{A}}{\partial t} = \boldsymbol{v} \wedge \boldsymbol{B} - \nabla \varphi, \tag{2.12}$$

where $\varphi(\boldsymbol{x}, t)$ is a scalar field satisfying

$$\nabla^2 \varphi = \nabla \cdot (\boldsymbol{v} \wedge \boldsymbol{B}). \tag{2.13}$$

Note that the 'gauge' of $\boldsymbol{A}$ may be changed by the replacement $\boldsymbol{A} \to \boldsymbol{A} + \nabla \chi$ for arbitrary scalar χ. The equation $\nabla \cdot \boldsymbol{A} = 0$ implies a particular choice of gauge. Equations (2.9) and (2.12) may be written in equivalent Lagrangian form:

$$\frac{\mathrm{D}}{\mathrm{D}t}\left(\frac{\boldsymbol{B}}{\rho}\right) = \frac{\boldsymbol{B}}{\rho} \cdot \nabla \boldsymbol{v}, \qquad \frac{\mathrm{D}A_i}{\mathrm{D}t} = v_j \frac{\partial A_j}{\partial x_i} - \frac{\partial \varphi}{\partial x_i}. \tag{2.14}$$

This form is most convenient for the proof of conservations of magnetic helicity, defined as follows: let S be any closed 'magnetic surface', i.e. a surface on which $\boldsymbol{B} \cdot \boldsymbol{n} = 0$, and let V be the (material) volume inside S. Then the magnetic helicity $\mathscr{H}_M$ in V is defined by

$$\mathscr{H}_M = \int \boldsymbol{A} \cdot \boldsymbol{B} \, \mathrm{d}V, \tag{2.15}$$

a pseudo-scalar quantity that may easily be shown to be independent of the gauge of $\boldsymbol{A}$. In the limit $\eta = 0$, this quantity is conserved (Woltjer 1958); for

$$\frac{\mathrm{d}}{\mathrm{d}t} \int \boldsymbol{A} \cdot \boldsymbol{B} \, \mathrm{d}V = \int \frac{\mathrm{D}\boldsymbol{A}}{\mathrm{D}t} \cdot \boldsymbol{B} \, \mathrm{d}V + \int \boldsymbol{A} \cdot \frac{\mathrm{D}}{\mathrm{D}t}\left(\frac{\boldsymbol{B}}{\rho}\right) \rho \, \mathrm{d}V, \tag{2.16}$$

and, using (2.14), this readily gives

$$\begin{aligned} \frac{\mathrm{d}}{\mathrm{d}t} \int \boldsymbol{A} \cdot \boldsymbol{B} \mathrm{d}V &= \int \nabla \cdot [\boldsymbol{B}(\boldsymbol{v} \cdot \boldsymbol{A} - \varphi)] \, \mathrm{d}V \\ &= \int_S (\boldsymbol{n} \cdot \boldsymbol{B})(\boldsymbol{v} \cdot \boldsymbol{A} - \varphi) \mathrm{d}S = 0. \end{aligned} \tag{2.17}$$

Note that this result holds whether the fluid is incompressible or not; it merely requires that the fluid be perfectly conducting.

This invariant admits interpretation in terms of linkage of the $\boldsymbol{B}$-lines (which are frozen in the fluid) (Moffatt 1969). To see this, consider the simplest 'prototype' linkage (figure 1) for which $\boldsymbol{B}$ is zero except in two flux

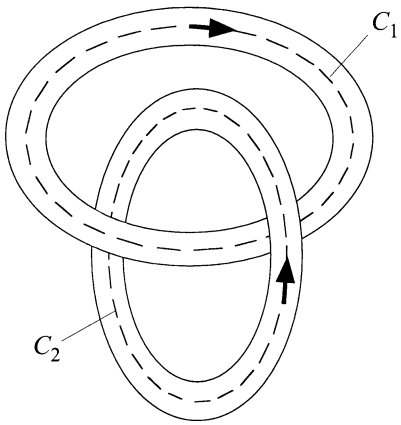

Figure 1. Linked flux tubes; here the linkage is right-handed and the linking number $n = 1$.

tubes of small cross-section centred on (unknotted) curves C_1 and C_2; the field lines within each tube are supposed to be unlinked, one with another. The sole linkage is then that between the two tubes, or equivalently between C_1 and C_2. Let Φ_1 and Φ_2 be the fluxes of $\boldsymbol{B}$ within these two tubes. The integral (2.16) may then be simply evaluated; it degenerates to

$$\mathscr{H}_M = \Phi_1 \oint_{C_1} \boldsymbol{A} \cdot \mathrm{d}\boldsymbol{x} + \Phi_2 \oint_{C_2} \boldsymbol{A} \cdot \mathrm{d}\boldsymbol{x}. \tag{2.18}$$

The two line integrals are zero if C_1 and C_2 are unlinked (more strictly if the flux of $\boldsymbol{B}$ across any surface spanning either C_1 or C_2 is zero); if C_1 and C_2 are linked, with linking number n, then, from (2.18)

$$\mathscr{H}_M = \pm 2n\Phi_1\Phi_2, \tag{2.19}$$

where the + or − is chosen according to whether the linkage is positive or negative; thus, for example, it is positive in figure 1, in which the sense of relative rotation is right-handed; if either arrow is reversed then the sign changes.

In general, $\boldsymbol{B}$-lines are not closed curves, and the above simple interpretation of $\mathscr{H}_M$ is not available. Nevertheless, $\mathscr{H}_M$ does always carry some limited information about the topology of the magnetic field (Arnold 1974; see also Arnold & Khesin 1998). This will be further considered in §6 below.

3 The Lorentz force and the equation of motion

As indicated in the introduction, the Lorentz force in the fluid (per unit volume) is $\boldsymbol{F} = \boldsymbol{j} \wedge \boldsymbol{B}$. With $\boldsymbol{j} = \mu_0^{-1} \nabla \wedge \boldsymbol{B}$, this admits alternative expression in terms of the Maxwell stress tensor

$$F_i = \frac{1}{\mu_0} \frac{\partial}{\partial x_j} \left(B_i B_j - \tfrac{1}{2} \boldsymbol{B}^2 \delta_{ij} \right) . \tag{3.1}$$

The first contribution, which may equally be written $\mu_0^{-1}(\boldsymbol{B} \cdot \nabla)\boldsymbol{B}$, represents a contribution to the force associated with curvature of $\boldsymbol{B}$-lines directed towards the centre of curvature; the second contribution, which may be written $-(2\mu_0)^{-1} \nabla \boldsymbol{B}^2$, represents (minus) the gradient of 'magnetic pressure'

$$p_M = (2\mu_0)^{-1} \boldsymbol{B}^2 . \tag{3.2}$$

In an incompressible fluid of constant density ρ, the equation of motion including these contributions to the Lorentz force may be written in the form

$$\frac{\partial \boldsymbol{v}}{\partial t} + \boldsymbol{v} \cdot \nabla \boldsymbol{v} = -\nabla \chi + \frac{1}{\mu_0 \rho} \boldsymbol{B} \cdot \nabla \boldsymbol{B} + \nu \nabla^2 \boldsymbol{v} , \tag{3.3}$$

where

$$\chi = (p + p_M)/\rho , \tag{3.4}$$

and ν is the kinematic viscosity of the fluid. Coupled with the induction equation (2.4) and appropriate boundary conditions, this determines the evolution of the fields $\{\boldsymbol{v}(\boldsymbol{x}, t), \boldsymbol{B}(\boldsymbol{x}, t)\}$.

We may illustrate this with reference to a phenomenon of central importance in MHD, namely the ability of the medium to support transverse wave motions in the presence of a magnetic field.

3.1 Alfvén waves

Suppose that the medium is of infinite extent, and that we perturb about a state of rest in which the fluid is permeated by a uniform magnetic field $\boldsymbol{B}_0$. Let $\boldsymbol{v}(\boldsymbol{x}, t)$ and $\boldsymbol{B} = \boldsymbol{B}_0 + \boldsymbol{b}(\boldsymbol{x}, t)$ be the perturbed velocity and magnetic fields. Then with the notation

$$\boldsymbol{V} = (\mu_0 \rho)^{-1/2} \boldsymbol{B}_0 , \qquad \boldsymbol{h} = (\mu_0 \rho)^{-1/2} \boldsymbol{b} , \tag{3.5}$$

the linearized forms of equations (2.4) and (3.3) (neglecting squares and products of $\boldsymbol{v}$ and $\boldsymbol{b}$) are

$$\left.\begin{aligned} \partial \boldsymbol{v}/\partial t &= -\nabla \chi + \boldsymbol{V} \cdot \nabla \boldsymbol{h} + \nu \nabla^2 \boldsymbol{v} , \\ \partial \boldsymbol{h}/\partial t &= (\boldsymbol{V} \cdot \nabla)\boldsymbol{v} + \eta \nabla^2 \boldsymbol{h} . \end{aligned}\right\} \tag{3.6}$$

These equations admit wave-like solutions with $\chi = \text{const.}$ and

$$\{\boldsymbol{v},\ \boldsymbol{h}\} \propto \mathrm{e}^{\mathrm{i}(\boldsymbol{k}\cdot\boldsymbol{x}-\omega t)} \tag{3.7}$$

provided

$$\left.\begin{aligned}(-\mathrm{i}\omega + \nu k^2)\boldsymbol{v} &= \mathrm{i}(\boldsymbol{k}\cdot\boldsymbol{V})\boldsymbol{h},\\ (-\mathrm{i}\omega + \eta k^2)\boldsymbol{h} &= \mathrm{i}(\boldsymbol{k}\cdot\boldsymbol{V})\boldsymbol{v}.\end{aligned}\right\} \tag{3.8}$$

Hence, for a non-trivial solution,

$$(\mathrm{i}\omega - \nu k^2)(\mathrm{i}\omega - \eta k^2) = -(\boldsymbol{k}\cdot\boldsymbol{V})^2, \tag{3.9}$$

which is a quadratic equation for ω with roots

$$\omega = -\tfrac{1}{2}\mathrm{i}(\eta + \nu)k^2 \pm \tfrac{1}{2}\left\{4(\boldsymbol{k}\cdot\boldsymbol{V})^2 - (\eta - \nu)^2k^4\right\}^{1/2}. \tag{3.10}$$

In the ideal-fluid limit ($\eta = 0,\ \nu = 0$), the roots are real:

$$\omega = \pm(\boldsymbol{k}\cdot\boldsymbol{V}), \tag{3.11}$$

a dispersion relationship of remarkable simplicity. Note that the group velocity associated with these waves is

$$\boldsymbol{c}_g = \nabla_{\boldsymbol{k}}\omega = \pm\boldsymbol{V}, \tag{3.12}$$

a result evidently independent of the wave-vector $\boldsymbol{k}$. The associated non-dispersive waves are known, after their discoverer, as Alfvén waves, and the velocity $\boldsymbol{V}$ is the Alfvén velocity (Alfvén 1950).

When $\eta + \nu \neq 0$, these waves are invariably damped. In the liquid-metal context, the damping is predominantly due to magnetic resistivity ($\eta \gg \nu$); if, moreover, the field $\boldsymbol{B}_0$ is strong in the sense that $|\boldsymbol{k}\cdot\boldsymbol{V}| \gg \eta^2k^4$, then (3.8) approximates to

$$\omega \approx -\tfrac{1}{2}\mathrm{i}\eta k^2 \pm \boldsymbol{k}\cdot\boldsymbol{V}, \tag{3.13}$$

and the nature of the damping is clear.

If, on the other hand, $|\boldsymbol{k}\cdot\boldsymbol{V}| \ll \eta^2k^4$, then the two roots (3.8) approximate to

$$\omega \approx -\mathrm{i}\eta k^2,\ -\mathrm{i}(\boldsymbol{k}\cdot\boldsymbol{V})^2/\eta k^2. \tag{3.14}$$

Now waves do not propagate, both modes are damped, and the first mode is damped much more rapidly than the second. Filtering of the first mode from equations (3.6) may be achieved by simply dropping the term $\partial\boldsymbol{h}/\partial t$; in this approximation, the field perturbation $\boldsymbol{h}$ is instantaneously determined by the flow $\boldsymbol{v}$.

4 Electromagnetic shaping and stirring

4.1 Two historic experiments

Two early papers provide examples of the manner in which applied magnetic fields and/or currents may contribute to the shaping of the region occupied by a conducting fluid and to the stirring of the fluid within this region. The first is that of Northrup (1907) who described an experiment in which a steady current is passed through a layer of conducting liquid (sodium–potassium alloy NaK) covered by a layer of (non-conducting) oil. The configuration described by Northrup is shown, in plan and elevation, in figure 2. The steady current $\boldsymbol{j}(\boldsymbol{x})$ passes through a constriction between two electrodes on the boundary; the increased current density in this region gives rise to an increased magnetic field encircling the current lines (via Ampere's Law); the resulting Lorentz force distribution causes depression of the oil/NaK interface. Northrup attributes this observation to his friend Carl Hering who, he says, "jocosely called it the 'pinch phenomenon' ". The famous 'pinch effect' is precisely the effect of contraction of a (compressible) cylindrical column of fluid carrying an axial current due to the self-induced radial magnetic pressure gradient, a behaviour of fundamental importance in plasma containment devices (figure 3); as Northrup and Hering recognized, a similar effect occurs even in liquid metals under experimentally realizable laboratory conditions. In the complex geometry of figure 2, the nonlinear deformation (i.e. shaping) of the interface is determined by a balance between Lorentz forces, gravity and surface tension; this is too complex to be calculated analytically, and numerical techniques would be required to solve this type of three-dimensional problem.

Northrup also commented that the liquid on the inclined surface of the interface 'showed great agitation'. This is a manifestation of the stirring effect, which, as will be shown below, inevitably accompanies the shaping influence of the magnetic field.

The second historic experiment is that described by Braunbeck (1932) and illustrated in figure 4. Here, a cylindrical capsule containing liquid metal is suspended on a torsion wire, and is subjected to a *rotating* magnetic field, as indicated. Such a field may be regarded as the superposition of two alternating fields in quadrature and at right angles, and may be easily produced using a three-phase power supply. Braunbeck observed that the capsule rotated in the direction of rotation of the field, achieving an equilibrium angle of rotation depending on the conductivity of the liquid; the device may thus in principle be calibrated to determine the conductivity of small samples of liquid metal. What is happening in equilibrium is that the liquid

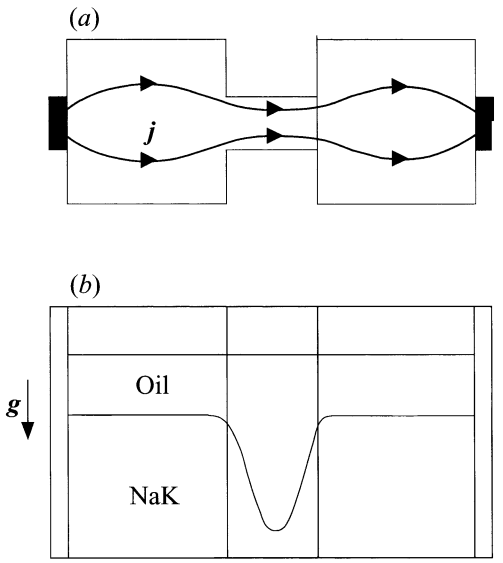

Figure 2. Sketch of Northrup's (1907) experiment: current flows through the NaK under a layer of oil; the constriction leads to a Lorentz force distribution which depresses the oil/NaK interface. (*a*) Plan; (*b*) elevation.

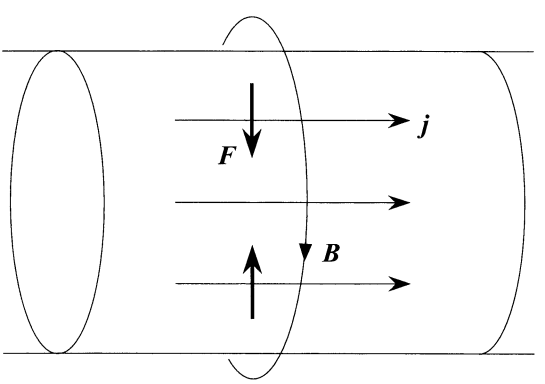

Figure 3. The pinch effect: axial current in the cylinder generates an azimuthal magnetic field; the resulting magnetic pressure gradient causes radial contraction of the cylinder.

metal rotates within the stationary container, exerting on it a viscous torque which is balanced by the restoring torque transmitted by the torsion wire. We shall analyse the details of this flow, and describe certain limitations of the description, below. Here, we may simply say that the stirring effect of an alternating or rotating magnetic field is a fundamental mechanism that is

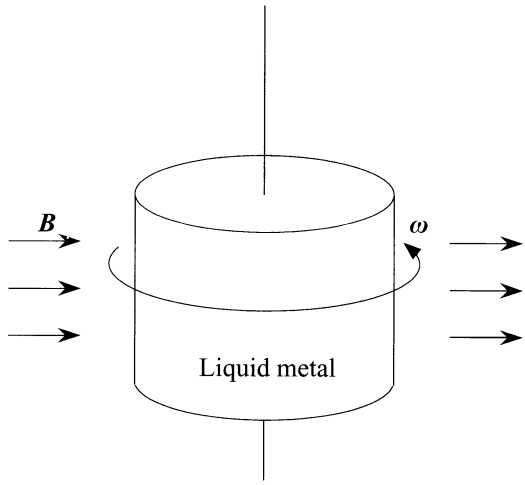

Figure 4. Sketch of the experiment of Braunbeck (1932): a capsule, containing liquid metal and suspended on a torsion wire, is subjected to a rotating magnetic field. This induces rotation in the fluid; the viscous torque on the capsule is then in equilibrium with the torque transmitted by the wire.

widely exploited in liquid-metal technology; thus, for example, it is used in the continuous casting of steel to stir the melt before solidification in order to produce a more homogeneous end-product (see, for example, Moffatt & Proctor 1984).

4.2 Electrically induced stirring

Northrup's problem as described above is one of a general class of problems in which a steady current distribution $\boldsymbol{j}(\boldsymbol{x})$ is established in the fluid in a domain $\mathscr{D}$ through prescription of an electrostatic potential distribution $\varphi_S(\boldsymbol{x})$ on the boundary S of this domain. This current, together with any external current closing the circuit, is the source for the magnetic field $\boldsymbol{B}(\boldsymbol{x})$, and flow is driven by the force $\boldsymbol{F} = \boldsymbol{j} \wedge \boldsymbol{B}$. If $R_m \ll 1$, then additional (induced) currents are weak, i.e. $\boldsymbol{j}(\boldsymbol{x})$ is effectively the same as if the conductor were at rest. Hence $\boldsymbol{j}$ is determined through solution of a Dirichlet problem:

$$\boldsymbol{j} = -\sigma \nabla \varphi, \tag{4.1}$$

where

$$\nabla^2 \varphi = 0 \text{ in } \mathscr{D}, \qquad \varphi = \varphi_S(\boldsymbol{x}) \quad \text{on} \quad S, \tag{4.2}$$

and $\boldsymbol{B}(\boldsymbol{x})$ is then given by (2.1).

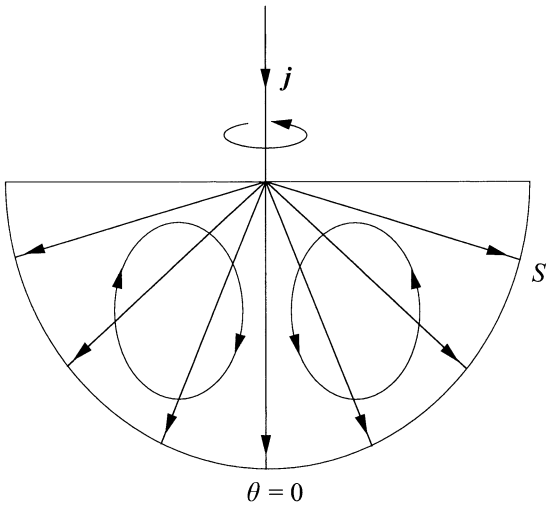

Figure 5. The weldpool problem: the Lorentz force drives the fluid towards the axis $\theta = 0$ and a strong jet flow develops along this axis; the flow is subject to instability involving swirl about this axis (Bojarevičs *et al.* 1989).

If the boundary S is entirely rigid, then the electromagnetic problem thus defined is conveniently decoupled from the fluid dynamical problem, and may be solved, either analytically or numerically, as a preliminary to determination of the force field $\boldsymbol{F}$ and the resulting flow field $\boldsymbol{v}$. If, on the other hand, as in Northrup's problem, part of the surface S is an interface with another fluid (usually non-conducting) then the dynamical problem of determining the shape of S is coupled with the electromagnetic problem of determining $\boldsymbol{j}$ and $\boldsymbol{B}$, an altogether more complex situation. Two problems of practical importance, described in the following subsections, have attracted much interest.

4.2.1 The weldpool problem

Here, current is injected through a point electrode at the surface S; the current spreads out radially (figure 5), and the configuration is locally axisymmetric about the direction of injection. Both $\boldsymbol{j}$ and $\boldsymbol{B}$ are singular at the point of injection, but of course these singularities are removed if the finite size of any real electrode is allowed for. Even so, the solution to this problem has some curious features that deserve comment here; for extended discussion, see Bojarevičs *et al.* (1989).

With local spherical polar coordinates (r, θ, φ) as indicated in figure 5, the

current in the fluid is given by

$$\boldsymbol{j} = (J/2\pi r^2, 0, 0) \tag{4.3}$$

and the corresponding field $\boldsymbol{B}$ is then given by

$$\boldsymbol{B} = \left(0, 0, \frac{\mu_0 J \sin\theta}{2\pi r(1+\cos\theta)}\right). \tag{4.4}$$

Note the singularities at $r = 0$. The Lorentz force is given by

$$\boldsymbol{F} = \boldsymbol{j} \wedge \boldsymbol{B} = \left(0, \frac{-\mu_0 J^2}{4\pi^2 r^3} \frac{\sin\theta}{1+\cos\theta}, 0\right). \tag{4.5}$$

This force, directed towards the axis $\theta = 0$, tends to drive the fluid towards this axis; being incompressible, the fluid has no alternative but to flow out along the axis in the form of a strong axisymmetric jet, which becomes increasingly 'focused' for decreasing values of the fluid viscosity.

Experimental realization of this flow indicates a behaviour that is not yet fully understood: the flow is subject to a strong symmetry-breaking instability in which the fluid spontaneously rotates, in one direction or the other, about the axial direction $\theta = 0$. It is believed that this rotation controls the singularity of axial velocity that otherwise occurs if the dimensionless parameter

$$K = \mu_0 J^2/\rho\nu^2 \tag{4.6}$$

exceeds a critical value K_c of order 300; a recent discussion of this perplexing phenomenon is given by Davidson *et al.* (1999).

4.2.2 Aluminium smelting

The essential ingredients of the industrial processes by which aluminium is extracted from the raw material cryolite (an electrolytic salt, sodium aluminium fluoride) are shown in figure 6. Current passes from the anodes to the cathode through the cryolite and a layer of molten aluminium grows from the cathode. There is now a jump of conductivity across the fluid/fluid interface so that the current lines are refracted across this interface. The magnetic field $\boldsymbol{B}$ is again that due to the current distribution in the fluids and the external circuit. The Lorentz force drives a flow in both fluids, the shape of the interface being controlled by gravity (surface tension effects being weak on the scale of this industrial process). The process is further complicated by instabilities of the interface to which the steady configuration may be subject (for detailed discussion, see Moreau 1990). This is a problem of enormous industrial importance: in effect the efficiency of the process is

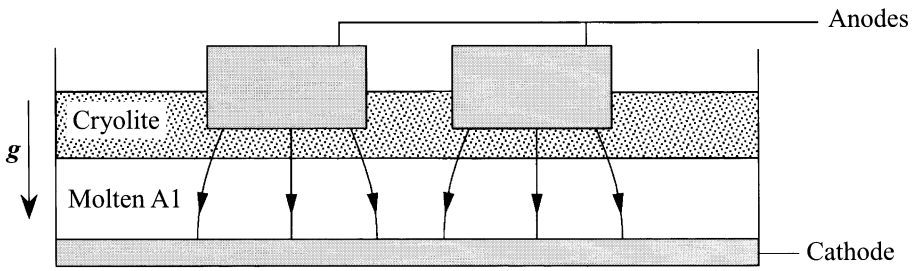

Figure 6. Sketch of the aluminium smelting process (Moreau 1990). The interface between the liquid cryolite and the molten aluminium is subject to instabilities of magnetohydrodynamic origin, which limit the efficiency of the process.

limited by instabilities that may lead to contact between the aluminium and the anodes, a 'short-circuiting' that would terminate the process. This is a billion-dollar industry for which an understanding of the fundamentals of magnetohydrodynamics would appear to be a first essential.

4.3 Inductive stirring

An equally important stirring mechanism is that associated with the application of an alternating (AC) magnetic field

$$\boldsymbol{B}(\boldsymbol{x},t) = \mathrm{Re}\left[\hat{\boldsymbol{B}}(\boldsymbol{x})\mathrm{e}^{-\mathrm{i}\omega t}\right], \tag{4.7}$$

such a field being produced by AC currents in external circuits (figure 7). The field diffuses into the conductor and a Lorentz force distribution $\boldsymbol{F}(\boldsymbol{x},t) = \boldsymbol{j}\wedge\boldsymbol{B}$ is established. This force distribution has a time-averaged part $\bar{\boldsymbol{F}}(\boldsymbol{x})$ and an additional periodic part with period 2ω and zero mean. The resulting flow consists of a steady part driven by $\bar{\boldsymbol{F}}(\boldsymbol{x})$, and a time-periodic part whose amplitude is controlled by the inertia of the fluid. We shall focus on the steady part in the present discussion, bearing in mind that this steady part may be unstable, in which case a turbulent response to the force $\bar{\boldsymbol{F}}(\boldsymbol{x})$ may be envisaged. We suppose that $R_m \ll 1$, so that again $\boldsymbol{B}(\boldsymbol{x},t)$ may be calculated as if the conductor were at rest.

4.3.1 The high-frequency limit

The qualitative nature of the force field $\bar{\boldsymbol{F}}(\boldsymbol{x})$ is best appreciated by first considering the high-frequency situation, in which $\boldsymbol{B}(\boldsymbol{x},t)$ is confined to a thin magnetic boundary layer (the skin effect) just inside the surface S. The

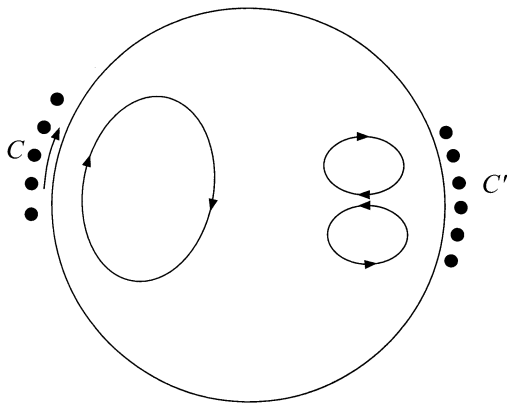

Figure 7. Stirring induced by AC fields; the sketch indicates the flow pattern that would be driven by a travelling magnetic field from the source coils C and a stationary AC field from the coils C; a wide range of patterns of stirring may be generated by appropriate engineering of the external coils and appropriate choice of field frequency ω.

thickness of this boundary layer is

$$\delta_M = (2\eta/\omega)^{1/2}, \tag{4.8}$$

and is small when ω is large. Outside the conductor, the field $\hat{\boldsymbol{B}}(\boldsymbol{x})$ is given by

$$\hat{\boldsymbol{B}} = \nabla\Phi, \qquad \nabla^2\Phi = 0, \tag{4.9}$$

and a boundary condition, which in the high-frequency limit is just

$$\partial\Phi/\partial n = 0 \quad \text{on} \quad S. \tag{4.10}$$

In effect, the field is perfectly excluded from the conductor in this limit. Of course, the potential Φ has 'prescribed' singularities at the external coils. Let us regard this 'external' problem as solved; then $\boldsymbol{B}_S = (\nabla\Phi)_S$ is known, as a tangential field on the surface S. Note that the surface divergence of $\boldsymbol{B}_S$ is non-zero in general; in fact

$$\nabla_S \cdot \boldsymbol{B}_S = -\frac{\partial B_n}{\partial n} = -\frac{\partial^2\Phi}{\partial n^2}\bigg|_S. \tag{4.11}$$

Within the skin inside the conductor, the field $\hat{\boldsymbol{B}}$ and hence $\hat{\boldsymbol{j}}$ can be calculated by standard methods; the mean force $\hat{\boldsymbol{F}} = \frac{1}{2}\mathrm{Re}(\hat{\boldsymbol{j}}^* \wedge \hat{\boldsymbol{B}})$ may then be found; here, the $*$ denotes the complex conjugate. Details may be found

in Moffatt (1985*b*); the result is

$$\boldsymbol{F} = \frac{1}{2\mu_0\delta_M}\left[|\boldsymbol{B}_S|^2\boldsymbol{n} - \mathrm{Im}\boldsymbol{B}_S^*(\nabla\cdot\boldsymbol{B}_S)\right]\mathrm{e}^{-2\zeta/\delta_M}, \tag{4.12}$$

where ζ is a normal coordinate directed into the conductor. The first term here is a strong inwardly directed normal component, which is responsible for the *shaping* of any part of S that is free to move in the normal direction. By contrast, *stirring* of the fluid is associated with the curl of $\boldsymbol{F}$, given by

$$\nabla\wedge\boldsymbol{F} = -\left(\frac{\rho}{\delta_M}\right)(\boldsymbol{n}\wedge\boldsymbol{Q}_S)\,\mathrm{e}^{-2\zeta/\delta_M}, \tag{4.13}$$

where

$$\boldsymbol{Q}_S = \frac{1}{\mu_0\rho}\left[\nabla_S\tfrac{1}{2}|\boldsymbol{B}_S|^2 - \mathrm{Im}\boldsymbol{B}_S^*\nabla_S\cdot\boldsymbol{B}_S\right], \tag{4.14}$$

a vector field defined on the surface S, and having the dimensions of an acceleration.

This force distribution will clearly generate a highly sheared flow within the boundary layer (thickness $O(\delta_M)$). We may estimate the net effect, on the reasonable assumption that fluid inertia is negligible compared with viscous effects within the layer. On this 'lubrication' assumption the velocity field within the layer, assuming a no-slip condition at $\zeta = 0$, is

$$\boldsymbol{v} = -\tfrac{1}{8}\delta_M^2\nu^{-1}\boldsymbol{Q}_S(\boldsymbol{x})\left(\mathrm{e}^{-2\zeta/\delta_M} - 1\right), \tag{4.15}$$

so that asymptotically

$$\boldsymbol{v} \sim \left(\delta_M^2/8\nu\right)\boldsymbol{Q}_S(\boldsymbol{x}) \quad \text{for} \quad \zeta \gg \delta_M. \tag{4.16}$$

What this means is that, under the influence of the magnetic field, the no-slip condition must be replaced by a condition of 'prescribed tangential velocity' as given by (4.16) for the driven flow in the interior of the conductor.

A corresponding analysis using a free-surface condition $\partial\boldsymbol{u}/\partial\zeta = 0$ on $\zeta = 0$ leads to an effective 'stress' condition

$$\tau_S = -\rho\nu\left(\partial\boldsymbol{u}/\partial\zeta\right)\big|_{\zeta=\infty} = \tfrac{1}{4}\rho\delta_M\boldsymbol{Q}_S(\boldsymbol{x}) \tag{4.17}$$

as a boundary condition for the interior flow. Note that this effective stress is independent of kinematic viscosity ν.

Thus, in the high-frequency limit, the influence of the magnetic field is confined to the magnetic boundary layer, or skin, in such a way as to simply replace the no-slip (or zero-stress) conditions on S by an effective slip (or effective stress) distribution on S, which is then responsible for generating an internal flow, a flow whose topology will clearly be influenced, and indeed

controlled, by the function $\boldsymbol{Q}_S(\boldsymbol{x})$, which is determined through (4.14) by the surface field $\boldsymbol{B}_S(\boldsymbol{x})$.

As the frequency is decreased, the skin depth δ_M increases, and the above simple description ceases to be valid; the force distribution penetrates more and more into the interior of the fluid, and extends throughout the fluid when δ_M increases to the scale L of the fluid domain.

4.3.2 The case of a circular cylinder

The prototype example is just as conceived by Braunbeck (1932): a horizontal rotating field applied to a circular cylinder with axis vertical and containing conducting fluid. Here,

$$\boldsymbol{B}_S = 2B_0 \mathrm{e}^{\mathrm{i}\theta} \boldsymbol{e}_\theta, \tag{4.18}$$

where B_0 is the value of field magnitude far from the cylinder, and θ is the angular coordinate. Hence, in this case, $|\boldsymbol{B}_S|^2$ is uniform on S, and

$$\nabla_S \cdot \boldsymbol{B}_S = \frac{2\mathrm{i}}{a} B_0 \mathrm{e}^{\mathrm{i}\theta} \quad \text{on} \quad S. \tag{4.19}$$

Hence, from (4.14) and (4.15), the effective slip velocity just inside the skin is

$$\boldsymbol{v} \approx \left(\eta B_0^2/\mu_0 \rho \omega \nu a\right) \boldsymbol{e}_\theta. \tag{4.20}$$

The resulting motion is a rigid body rotation of the fluid inside this skin, with angular velocity

$$\Omega = \eta B_0^2/\mu_0 \rho \omega \nu a^2, \tag{4.21}$$

a result obtained originally by Moffatt (1965). The viscous stress and resulting couple G (per unit length of cylinder) acting on the cylinder are easily calculated, with the result

$$G = 2\pi \left(\frac{2\eta}{\omega}\right)^{1/2} \frac{B_0^2}{\mu_0 \rho}. \tag{4.22}$$

Remarkably, this couple, although of viscous origin, is independent of ν; this is because the core angular velocity, given by (4.21), is proportional to ν^{-1}. In Braunbeck's experiment, it is the torque (4.22) that is ultimately in equilibrium with the torque transmitted by the torsion wire, which is proportional to the net angle of rotation; thus measurement of this angle provides a means of determination of η, and hence of the conductivity σ.

There are of course a number of limitations of the above type of analysis that should be borne in mind. First, the high-frequency approximation is valid only if $\delta_M \ll a$, i.e. $\omega \gg \eta/a^2$. This is not however a serious restriction;

the problem can be solved exactly for arbitrary ω in terms of Bessel functions. More seriously however, the analysis fails if the field strength B_0 becomes so strong that Ω in (4.21) becomes comparable with ω; for it is in fact not the *absolute* angular velocity ω of the field that is relevant to the induction of currents, but rather the *relative* angular velocity $\omega - \Omega$ between field and fluid. This strong field situation requires a major modification of approach (see, for example, Moreau 1990, where problems of this type are extensively treated).

4.3.3 Magnetic levitation

A high-frequency field also offers the possibility of levitating a volume (usually a small droplet) of conducting liquid in the complete absence of any rigid boundary support (figure 8); here, it may be more appropriate to talk of a magnetic basket rather than a magnetic bottle! The field is again expelled from the conductor (except in a thin skin); the first contribution to the force $\boldsymbol{F}$ in (4.12) corresponds to the effect of magnetic pressure p_M on the surface S; if S can so adjust itself that each vertical column of liquid of length Δz is support by the magnetic pressure difference Δp_M between bottom and top, i.e.

$$\Delta p_M = \rho g \Delta z\,, \tag{4.23}$$

then levitation is possible. This can be achieved by placing the main current sources of the field $\boldsymbol{B}$ *below* the liquid sample as in the configuration envisaged in figure 8(*a*). In the axisymmetric configuration of figure 8(*b*), the magnetic pressure vanishes on the axis of symmetry, and (4.23) cannot be satisfied; one must rely on surface tension to compensate gravity for the column of fluid immediately adjacent to this axis.

Configurations of this kind have been studied in some detail by Mestel (1982) and by Sneyd & Moffatt (1982). As pointed out in the latter paper, the effective stress given by (4.17) drives an interior flow with closed streamlines, whose intensity is limited only by viscosity. This is because integration of the steady equation of motion in the form

$$0 = \boldsymbol{v} \wedge \boldsymbol{\omega} - \nabla\left(\frac{p}{\rho} + \tfrac{1}{2}\boldsymbol{v}^2\right) + \boldsymbol{F} - \nu \nabla \wedge \boldsymbol{\omega} \tag{4.24}$$

round a closed streamline C gives

$$\oint_C \boldsymbol{F} \cdot \mathrm{d}\boldsymbol{x} = \nu \oint_C \mathrm{d}\boldsymbol{x} \cdot (\nabla \wedge \boldsymbol{\omega})\,, \tag{4.25}$$

i.e. inertia and pressure forces play no part in the equilibrium that is established. In practice, the viscosity in liquid metals is small; put another way,

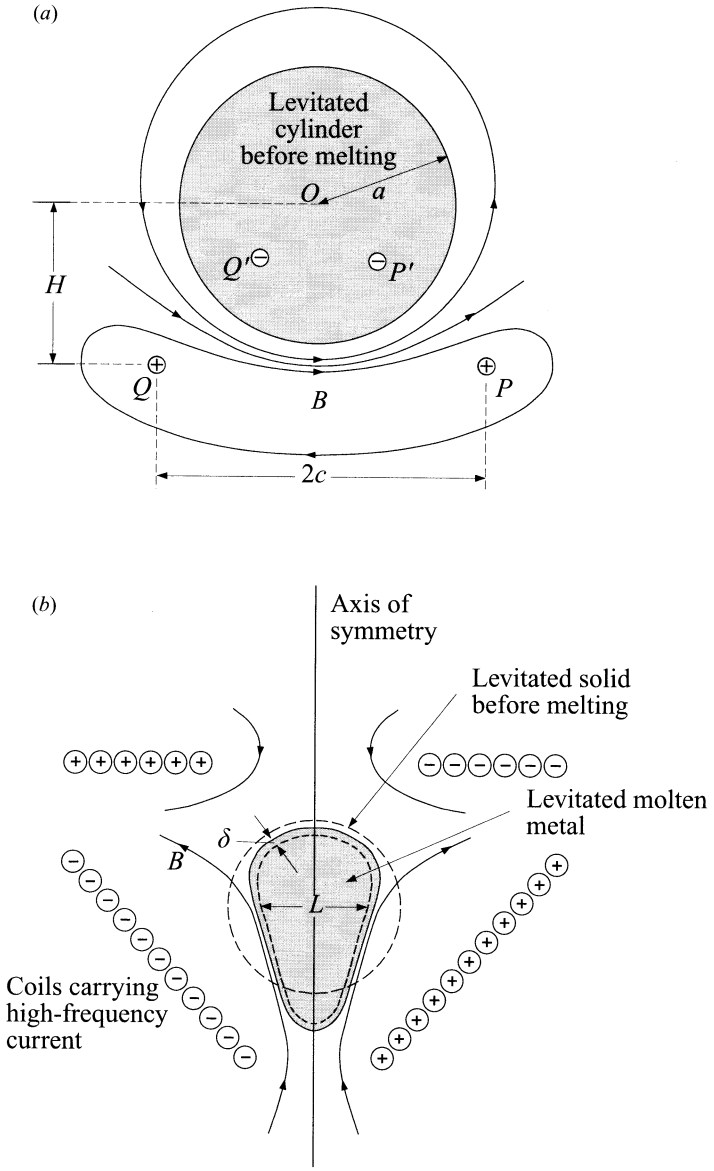

Figure 8. Magnetic levitation by high-frequency magnetic field, providing support via magnetic pressure distribution on the surface (Sneyd & Moffatt 1982).

the Reynolds number of the flow that is necessarily driven in the interior of a levitated droplet of radius of the order of 10 mm or greater is very large. It seems likely therefore that this interior flow will in these circumstances be turbulent. The 'great agitation' referred to by Northrup (see § 4.1 above) also

presumably indicated a state of turbulent flow just inside the liquid metal – and for similar reasons.

5 Dynamo theory

Dynamo theory is concerned with explaining the origin of magnetic fields in stars, planets and galaxies. Such fields are produced by currents in the interior regions, which would in the normal course of events be subject to ohmic decay, in the same way that current in an electric circuit decays if not maintained by a battery. This decay can however be arrested, and indeed reversed, through inductive effects associated with fluid motion; when this happens, the fluid system acts as a self-exciting dynamo. The magnetic field grows spontaneously from an arbitrary weak initial level, in much the same way as any other perturbation of an intrinsically unstable situation.

The possibility of such 'dynamo' instabilities may be understood with reference to the induction equation (2.4), which governs field evolution if the velocity field $\boldsymbol{v}(\boldsymbol{x}, t)$ in the fluid is regarded as 'given'. Let us suppose for simplicity that the fluid fills all space, and that the velocity field is steady, i.e. $\boldsymbol{v} = \boldsymbol{v}(\boldsymbol{x})$. We must suppose also that $\boldsymbol{B}$ has no 'sources at infinity' which would mitigate against the concept of an internally generated dynamo.

We may seek 'normal mode' solutions of (2.4) of the form

$$\boldsymbol{B}(\boldsymbol{x}, t) = \mathrm{Re}\left[\hat{\boldsymbol{B}}(\boldsymbol{x})\, \mathrm{e}^{pt}\right], \tag{5.1}$$

where, by substitution,

$$p\hat{\boldsymbol{B}} = \nabla \wedge (\boldsymbol{v} \wedge \hat{\boldsymbol{B}}) + \eta \nabla^2 \hat{\boldsymbol{B}}. \tag{5.2}$$

When coupled with the requirement that $\hat{\boldsymbol{B}}(\boldsymbol{x})$ should be either a localized field of finite energy or, for example, a space-periodic field if $\boldsymbol{v}$ is space-periodic, this constitutes an eigenvalue problem which (in principle) determines a sequence of possibly complex eigenvalues $p_1, p_2, \ldots$, which may be ordered so that

$$\mathrm{Re}\, p_1 \geqslant \mathrm{Re}\, p_2 \geqslant \mathrm{Re}\, p_3 \geqslant \ldots, \tag{5.3}$$

and corresponding 'eigenfields' $\hat{\boldsymbol{B}}_1(\boldsymbol{x}), \hat{\boldsymbol{B}}_2(\boldsymbol{x}), \ldots$. If $\mathrm{Re}\, p_1 > 0$, then the corresponding field

$$\boldsymbol{B}(\boldsymbol{x}, t) = \mathrm{Re}\left[\hat{\boldsymbol{B}}_1(\boldsymbol{x})\, \mathrm{e}^{p_1 t}\right] \tag{5.4}$$

exhibits dynamo behaviour: it grows exponentially in intensity, the growth

being oscillatory or non-oscillatory according to whether $\mathrm{Im}\, p_1 \neq 0$ or $= 0$. The mode of maximum growth-rate is clearly the one that will emerge from an arbitrary initial condition in which all modes may be present.

If this exponential growth occurs, then it can persist only for as long as the velocity field $\boldsymbol{v}(\boldsymbol{x})$ remains unaffected by the Lorentz force. This is the 'kinematic phase' of the dynamo process. Obviously, however, the Lorentz force increases exponentially with growth rate $2\mathrm{Re}\, p_1$ (considering only the mode (5.4)) and so ultimately the back-reaction of the Lorentz force on the fluid motion must be taken into account. This is the 'dynamic phase' of dynamo action in which the nature of the supply of energy to the system (via the dynamic equation of motion) must be considered. While great progress has been made over the past 50 years towards a full understanding of the kinematic phase, the highly nonlinear dynamic phase has proved far more intractable from an analytical point of view, and is likely to remain a focus of much research effort, both computational and analytical, over the next few decades.

5.1 Fast and slow dynamos

During the kinematic phase, the growth rate (p say) of the most unstable mode is determined in principle by the velocity field $\boldsymbol{v}(\boldsymbol{x})$ and the parameter η which appears in equation (5.2). If $\boldsymbol{v}(\boldsymbol{x})$ is characterized by velocity scale v_0 and length scale l_0, then on dimensional grounds,

$$p = (v_0/l_0) f(R_m), \tag{5.5}$$

where, as in § 2.1, $R_m = v_0 l_0/\eta$. An important distinction between dynamos described as 'fast' or 'slow' has been introduced by Vainshtein & Zel'dovich (1972). A fast dynamo is one for which $f(R_m) = O(1)$ as $R_m \to \infty$, i.e. the growth rate p scales on the dynamic time scale l_0/v_0. A slow dynamo, by contrast, is one for which $f(R_m) \to 0$ as $R_m \to \infty$; for example, if $f(R_m) \sim R_m^{-1/2}$ as $R_m \to \infty$, then $p \sim (v_0/l_0) R_m^{-1/2}$, and diffusivity η continues to influence the growth rate even in the limit $\eta \to 0$. The distinction is an important one because, on the galactic scale, R_m is extremely large, and a slow dynamo is likely to have little relevance in such contexts. This has led to an intensive search for dynamos that can legitimately be described as fast (see Childress & Gilbert 1995); however, in the strict sense indicated above, no such dynamo has yet been found! All known dynamos are slow; diffusivity remains important no matter how small η may be. The situation is again somewhat analogous to that governing the vorticity equation in turbulent flow: viscous effects remain important (in providing the mechanism for

dissipation of kinetic energy) no matter how small the kinematic viscosity ν may be.

When a dynamo enters the dynamic phase (assuming that sufficient time is available for it to do so) the distinction between fast and slow behaviour disappears; in either case, the growth rate must decrease, ultimately to zero when an equilibrium between generation of magnetic field by the (modified) velocity field and ohmic dissipation of magnetic field is established.

5.2 A little historical digression

The history of dynamo theory up to 1957, when Cowling's seminal monograph *Magnetohydrodynamics* was published, was characterized by the gravest uncertainty as to whether any form of self-exciting dynamo action in a spherical body of fluid of uniform conductivity was possible at all. One of the main firm results in this regard was negative: this was Cowling's (1934) theorem, which stated in its simplest form that steady axisymmetric dynamo action is impossible. This reinforced the view prevalent at the time, and originally stated in the geomagnetic context by Schuster (1912) that 'the difficulties which stand in the way of basing terrestrial magnetism on electric currents inside the earth are insurmountable'. Fortunately this pessimistic conclusion has been eroded and now completely reversed with the passage of time. For example, Cook (1980) writes that 'there is no theory other than a dynamo theory that shows any sign of accounting for the magnetic fields of the planets'. This view is echoed by Jacobs (1984) who writes 'There has been much speculation on the origin of the Earth's magnetic field ... The only possible means seems to be some form of electromagnetic induction, electric currents flowing in the Earth's core'.

If we try to identify one single development over the last half-century that has revolutionized our view of the subject, that development must surely be the 'mean-field electrodynamics' proposed in the seminal paper of Steenbeck, Krause & Rädler (1966), and foreshadowed in earlier 'pre-seminal' papers of Parker (1955) and Braginski (1964). This theory, which led in the fully turbulent context to the discovery of the famous α-effect – the appearance of a mean electromotive force parallel to the mean magnetic field – lies at the heart of the dynamo process as currently understood. In effect, it provides a starting point for any modern approach to dynamo theory; as such, it merits the closest study. A simplified account is presented in the following sub-sections. A systematic treatment may be found in the research monographs of Moffatt (1978) and Krause & Rädler (1980). Extensive treatment, with particular reference to astrophysical application, may also

be found in the books of Parker (1979) and Zeldovich, Ruzmaikin & Sokoloff (1983).

5.3 Mean-field electrodynamics

Let us suppose that the velocity $\boldsymbol{v}(\boldsymbol{x}, t)$ appearing in equation (2.4) is turbulent – i.e. random in both space and time (see Chapter 5). We may suppose that there is some source of energy for this turbulence (e.g. through some random stirring mechanism) so that $\boldsymbol{v}$ is statistically stationary in time. It is then natural to adopt the notation $\langle \ldots \rangle$ for a time average, over any interval long compared with the time scale $t_0 = l_0/v_0$ characteristic of the energy-containing eddies of the turbulence; here l_0 is the scale of these eddies and v_0 the r.m.s. value of $\boldsymbol{v}$. For simplicity, we may suppose that $\langle \boldsymbol{v} \rangle = 0$.

The field $\boldsymbol{B}(\boldsymbol{x}, t)$ may be decomposed into mean and fluctuating parts:

$$\boldsymbol{B}(\boldsymbol{x}, t) = \boldsymbol{B}_0(\boldsymbol{x}, t) + \boldsymbol{b}(\boldsymbol{x}, t), \tag{5.6}$$

where $\boldsymbol{B}_0(\boldsymbol{x}, t) = \langle \boldsymbol{B}(\boldsymbol{x}, t) \rangle$ and $\langle \boldsymbol{b} \rangle \equiv 0$. Here we allow $\boldsymbol{B}_0$ to depend on t; this must be interpreted as allowing for slow evolution on a time scale T much greater than t_0. Separation of the time scales t_0 and T ($t_0 \ll T$) is the key to the solution of the problem. The theory may equally be developed in terms of separation of *spatial* scales l_0 and the scale $L (\gg l_0)$ on which the mean field develops.

The mean of equation (2.4) gives an evolution equation for $\boldsymbol{B}_0(\boldsymbol{x}, t)$:

$$\frac{\partial \boldsymbol{B}_0}{\partial t} = \nabla \wedge \boldsymbol{\mathcal{E}} + \eta \nabla^2 \boldsymbol{B}_0, \tag{5.7}$$

where $\boldsymbol{\mathcal{E}} = \langle \boldsymbol{v} \wedge \boldsymbol{b} \rangle$, the mean electromotive force arising through interaction of the fluctuating fields. Now the problem is like the 'closure' problem of turbulence: we need to find a relationship between $\boldsymbol{\mathcal{E}}$ and $\boldsymbol{B}_0$ in order to solve (5.7). But now, in contrast to the intractable problem of turbulence, we have the separation of scales to help us.

Subtracting (5.7) from (2.4) gives an equation for the fluctuating field $\boldsymbol{b}$:

$$\frac{\partial \boldsymbol{b}}{\partial t} = \nabla \wedge (\boldsymbol{v} \wedge \boldsymbol{B}_0) + \nabla \wedge (\boldsymbol{v} \wedge \boldsymbol{b} - \boldsymbol{\mathcal{E}}) + \eta \nabla^2 \boldsymbol{b}. \tag{5.8}$$

Without further approximation, it is difficult, if not impossible, to solve for $\boldsymbol{b}$ in terms of $\boldsymbol{B}_0$ and $\boldsymbol{v}$. However, we may make progress by noting that, for given $\boldsymbol{v}(\boldsymbol{x}, t)$, equation (5.8) establishes a linear relationship between $\boldsymbol{b}$ and $\boldsymbol{B}_0$; and hence, since $\boldsymbol{\mathcal{E}}$ is linearly related to $\boldsymbol{b}$, between $\boldsymbol{\mathcal{E}}$ and $\boldsymbol{B}_0$.

Now both $\boldsymbol{\mathcal{E}}$ and $\boldsymbol{B}_0$ are average fields varying on the slow time scale, and

on the large length scale L; hence this linear relationship between $\mathscr{E}$ and $\boldsymbol{B}_0$ may be represented by a series of the form

$$\mathscr{E}_i = \alpha_{ij} B_{0j} + \beta_{ijk} \frac{\partial B_{0j}}{\partial x_k} + \dots , \tag{5.9}$$

where $\alpha_{ij}, \beta_{ijk}, \dots$ are tensor (actually pseudo-tensor) coefficients which are in principle determined by the statistical properties of the turbulent field $\boldsymbol{v}(\boldsymbol{x}, t)$ and the parameter η which intervenes in the solution of (5.8). Note that successive terms of (5.9) decrease in magnitude by a factor of order l_0/L; and that any terms involving time derivatives, i.e. $\partial \boldsymbol{B}_0/\partial t$, may be eliminated in favour of space derivatives through recursive appeal to equation (5.7). That the coefficients $\alpha_{ij}, \beta_{ijk}, \dots$ are pseudo-tensors (rather than tensors) should be evident from the fact that $\mathscr{E}$ is a polar vector (like velocity) whereas $\boldsymbol{B}_0$ is an axial vector (like angular velocity).

We may go further on the simplifying assumption that the turbulence is homogeneous and isotropic. In this case, α_{ij} and β_{ijk} share these properties, i.e. they are isotropic pseudo-tensors invariant under translation, i.e. independent of $\boldsymbol{x}$ (they are already independent of t from the assumption that $\boldsymbol{v}$ is statistically stationary). Isotropy is a very strong constraint; it implies that

$$\alpha_{ij} = \alpha \delta_{ij} , \qquad \beta_{ijk} = \beta \epsilon_{ijk} \dots , \tag{5.10}$$

where now α is a pseudo-scalar quantity and β is a pure scalar. Hence (5.9) simplifies to

$$\mathscr{E} = \alpha \boldsymbol{B}_0 - \beta(\nabla \wedge \boldsymbol{B}_0) + \dots ; \tag{5.11}$$

the next term in this series involves $\nabla \wedge (\nabla \wedge \boldsymbol{B}_0)$ and so on. This is the required relationship between $\mathscr{E}$ and $\boldsymbol{B}_0$.

Substituting this back into (5.7) gives the mean-field equation in its simplest form:

$$\frac{\partial \boldsymbol{B}_0}{\partial t} = \alpha(\nabla \wedge \boldsymbol{B}_0) + (\eta + \beta)\nabla^2 \boldsymbol{B}_0 + \dots , \tag{5.12}$$

where the terms indicated by $+\dots$ involve higher derivatives of $\boldsymbol{B}_0$, and may presumably be neglected when the scale of variation of $\boldsymbol{B}_0$ is large. It is clear from the structure of (5.12) that β must be interpreted as an 'eddy diffusivity' associated with the turbulence (although there is no guarantee from the above treatment that β must invariably be positive!). The first term on the right of (5.12) will however always dominate the evolution, provided $\alpha \neq 0$ and the scale of $\boldsymbol{B}_0$ is sufficiently large. Before going further it is therefore essential to find a means of calculating α explicitly and determining the conditions under which this key parameter is definitely non-zero.

5.4 First-order smoothing

To do this, it is legitimate to consider the situation in which $\boldsymbol{B}_0$ is constant; the reason for this is that α is independent of the field $\boldsymbol{B}_0(\boldsymbol{x}, t)$, and we are free to make any assumption about this field that simplifies calculation of α. The assumption that $\boldsymbol{B}_0$ is constant is equivalent to considering the conceptual limit $L \to \infty$, $T \to \infty$.

Under this condition, the fluctuation equation (5.8) becomes

$$\frac{\partial \boldsymbol{b}}{\partial t} = (\boldsymbol{B}_0 \cdot \nabla)\boldsymbol{v} + \nabla \wedge (\boldsymbol{v} \wedge \boldsymbol{b} - \mathscr{E}) + \eta \nabla^2 \boldsymbol{b}. \tag{5.13}$$

Now we know that, if the magnetic Reynolds number $R_m = v_0 l_0/\eta$ is *small*, then the induced field $\boldsymbol{b}$ is weak compared with $\boldsymbol{B}_0$ (actually $\boldsymbol{b} = O(R_m)\boldsymbol{B}_0$; see below). In this circumstance, the awkward term $\nabla \wedge (\boldsymbol{v} \wedge \boldsymbol{b} - \mathscr{E})$ in (5.8) is negligible compared with the other terms in the equation and may be neglected. We then have a linear equation with constant coefficients which may be solved by elementary Fourier techniques. Let us then make this assumption and explore the consequences.

It is illuminating to consider first the situation in which $\boldsymbol{v}$ is a circularly polarized wave of the form

$$\boldsymbol{v}(\boldsymbol{x}, t) = v_0(\sin(kz - \omega t), \cos(kz - \omega t), 0), \tag{5.14}$$

and $\boldsymbol{B}_0 = (0, 0, B_0)$ (see figure 9). Note that the vorticity associated with (5.14) is

$$\boldsymbol{\omega} = \nabla \wedge \boldsymbol{v} = k\boldsymbol{v}, \tag{5.15}$$

and the associated helicity density,

$$\mathscr{H} = \boldsymbol{v} \cdot \boldsymbol{\omega} = k\boldsymbol{v}^2 = kv_0^2, \tag{5.16}$$

is maximal (since $\boldsymbol{\omega}$ is parallel to $\boldsymbol{v}$) and constant. Then we easily find that (5.13) is satisfied provided

$$\boldsymbol{b} = \frac{B_0 v_0 k}{\omega^2 + \eta^2 k^4} (\eta k^2 \cos\varphi - \omega \sin\varphi, -\omega \cos\varphi - \eta k^2 \sin\varphi, 0) \tag{5.17}$$

where $\varphi = kz - \omega t$. We then obtain

$$\boldsymbol{v} \wedge \boldsymbol{b} = \frac{-B_0 v_0^2 k^3 \eta}{\omega^2 + \eta^2 k^4}(0, 0, 1). \tag{5.18}$$

For this case of a single 'helicity' wave (5.14), $\boldsymbol{v} \wedge \boldsymbol{b}$ turns out to be uniform, so the awkward term in (5.13) is identically zero! It follows from (5.18) that

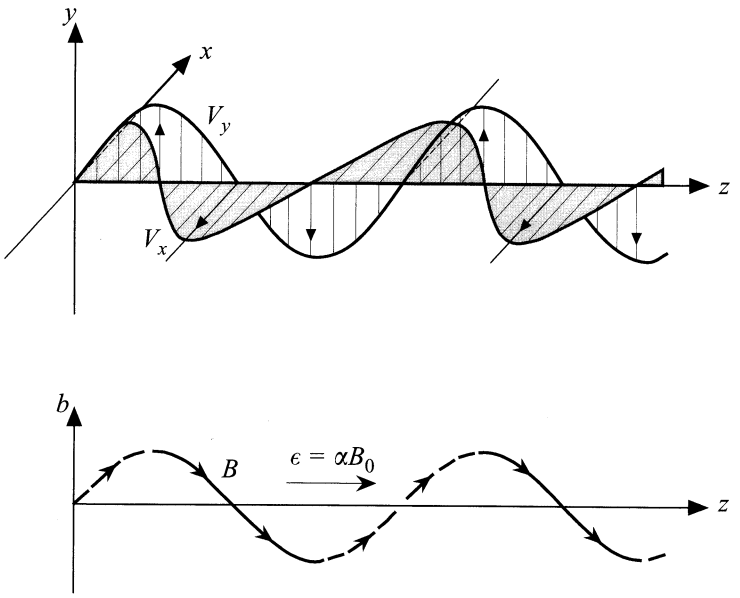

Figure 9. A circularly polarized travelling wave $\boldsymbol{v}(\boldsymbol{x}, t)$ of the form (5.14) induces and interacts with the field $\boldsymbol{b}$ which is also circularly polarized (equation (5.17)), but phase-shifted relative to $\boldsymbol{v}$. The resulting $\boldsymbol{v} \wedge \boldsymbol{b}$ is uniform and parallel to $\boldsymbol{B}_0$.

$\mathscr{E} = \alpha \boldsymbol{B}_0$, where

$$\alpha = -\frac{\eta k^2}{\omega^2 + \eta^2 k^4} \mathscr{H}. \tag{5.19}$$

It is obviously desirable to write the result in this form, both left- and right-hand sides of the equation being pseudo-scalars.

It is important to note the origin of the 'α-effect' contained in (5.19): it is the phase-shift between $\boldsymbol{b}$ and $\boldsymbol{v}$ caused by molecular diffusivity η which leads to a non-zero value for α; it is a strange fact that, although diffusion is responsible for the decay of magnetic field in the absence of fluid motion, it is also responsible for the appearance of an α-effect which, as shown below, is a vital ingredient of the self-exciting dynamo process.

The velocity field (5.14) is of course rather special; it should be clear however that if we consider a random superposition of such waves with wave-vectors $\boldsymbol{k}$, frequencies ω, and amplitudes $\hat{\boldsymbol{v}}(\boldsymbol{k}, \omega)$ isotropically distributed, then, provided the awkward term of (5.13) can be neglected, a result generalizing (5.19) can be obtained; all the contributions from different wave

modes are additive, and the final result is

$$\alpha = -\tfrac{1}{3}\eta \iint \frac{k^2 \mathscr{H}(\boldsymbol{k},\omega)\,\mathrm{d}^3\boldsymbol{k}\,\mathrm{d}\omega}{\omega^2 + \eta^2 k^4}, \tag{5.20}$$

where $\mathscr{H}(\boldsymbol{k},\omega)$ is the helicity spectrum function of the velocity field $\boldsymbol{v}$, with the property

$$\langle \boldsymbol{v}\cdot\boldsymbol{\omega}\rangle = \iint \mathscr{H}(\boldsymbol{k},\omega)\,\mathrm{d}^3\boldsymbol{k}\,\mathrm{d}\omega\,. \tag{5.21}$$

The factor $\frac{1}{3}$ appears in (5.20) from averaging over all directions. The main thing to note again is the direct relationship between α and the helicity of the turbulent field.

This theory, usually described as 'first-order smoothing' theory, is limited to circumstances in which, as indicated above, $|\boldsymbol{b}| \ll |\boldsymbol{B}_0|$. This condition is satisfied if $R_m \ll 1$; it is also satisfied under the alternative condition

$$|v_0 k/\omega| \ll 1 \tag{5.22}$$

for values of k and ω making the dominant contributions to the field of turbulence. The condition (5.22) is relevant in a rapidly rotating system in which the turbulence is more akin to a field of weakly interacting inertial waves whose frequencies ω are of the order of the angular velocity Ω of the system; in this context, the condition (5.22) is one of small Rossby number.

If neither of the above conditions is satisfied, then it is not legitimate to neglect the awkward term in (5.13); no fully satisfactory theory is as yet available for the determination of α in these circumstances. Nevertheless, one may assert that the key property of turbulence required to provide a non-zero value for α is that its statistical properties should *lack reflectional symmetry*, i.e. should be non-invariant under change from a right-handed to a left-handed frame of reference; it is this same property that is necessary to provide non-zero mean helicity $\mathscr{H} = \langle \boldsymbol{v}\cdot\boldsymbol{\omega}\rangle$, which is indeed a simple measure of 'lack of reflectional symmetry', and so a loose connexion between α and $\mathscr{H}$ is to be expected.

The concept of isotropic turbulence that lacks reflectional symmetry is quite novel! One often thinks of a turbulent vorticity field in pictorial terms as like a random field of spaghetti; to picture turbulence lacking reflectional symmetry, think rather of a pasta in which each pasta element is twisted with the same sense of twist – say right-handed: if the vorticity field follows the sense of these elements, it remains statistically isotropic but acquires positive helicity. For a more realistic example, it suffices to consider Bénard convection in a rotating system (see, for example, Chandrasekhar 1961); it

turns out that the average of $\boldsymbol{v} \cdot \boldsymbol{\omega}$ over horizontal planes is non-zero and antisymmetric about the centreplane (Moffatt 1978, chap. 10).

5.5 Dynamo action associated with the α-effect

Let us return now to the mean field equation (5.12) in the form

$$\frac{\partial \boldsymbol{B}}{\partial t} = \alpha \nabla \wedge \boldsymbol{B} + \eta_e \nabla^2 \boldsymbol{B}, \tag{5.23}$$

where now $\eta_e = \eta + \beta$ is the 'effective diffusivity', and we drop the suffix 0 on $\boldsymbol{B}_0$, to simplify notation. The simplest way to treat (5.23) is to seek solutions which have the Beltrami property

$$\nabla \wedge \boldsymbol{B} = K\boldsymbol{B}, \tag{5.24}$$

where K is a constant. For example, the field

$$\boldsymbol{B} = (c \sin Kz + b \cos Ky, a \sin Kx + c \cos Kz, b \sin Ky + a \cos Kx) \tag{5.25}$$

(the 'abc' field) has this property, as may be easily verified. We shall suppose that K is chosen to have the same sign as α, i.e. $\alpha K > 0$, and that $|K|$ is small, so that the scale $L \sim K^{-1}$ of $\boldsymbol{B}$ is large compared with the scale l_0 of the underlying turbulence that gives rise to the α-effect. Of course (5.23) implies that

$$\nabla^2 \boldsymbol{B} = -\nabla \wedge (\nabla \wedge \boldsymbol{B}) = -K^2 \boldsymbol{B}, \tag{5.26}$$

and so (5.23) becomes

$$\frac{\partial \boldsymbol{B}}{\partial t} = \left(\alpha K - \eta_e K^2\right) \boldsymbol{B}, \tag{5.27}$$

so that

$$\boldsymbol{B}(\boldsymbol{x}, t) = \boldsymbol{B}(\boldsymbol{x}, 0)\, \mathrm{e}^{pt}, \tag{5.28}$$

where

$$p = \alpha K - \eta_e K^2. \tag{5.29}$$

Obviously we have exponential growth of the mean field $\boldsymbol{B}$ provided $\alpha K > \eta_e K^2$, i.e. provided

$$|K| < |\alpha| / \eta_e. \tag{5.30}$$

Thus we have a dynamo effect, in which the mean field (i.e. the field on the large scale L) grows exponentially provided L is large enough.

If we adopt the low-R_m estimate for α (based on (5.20)),

$$\alpha \sim \frac{1}{\eta} l_0^2 \mathscr{H} \sim R_m v_0 \tag{5.31}$$

assuming $\mathscr{H} \sim v_0^2/l_0$, and note that in this low-R_m situation, $\beta \ll \eta$ (actually $\beta = O(R_m^2)\eta$), then the scale of maximum growth rate is given (from (5.29)) by

$$L \sim K^{-1} \sim R_m^{-2} l_0 . \tag{5.32}$$

Hence a new magnetic Reynolds number $\tilde{R}_m$ defined in terms of L rather than l_0 is given by

$$\tilde{R}_m = \frac{L v_0}{\eta} \sim R_m^{-2} R_m \sim R_m^{-1} . \tag{5.33}$$

The condition $R_m \ll 1$ implies that $\tilde{R}_m \gg 1$: the field grows on a scale L at which the corresponding $\tilde{R}_m$ is *large*.

We can now summarize the implications of the above discussion. If a conducting fluid is in turbulent motion, the turbulence being homogeneous and isotropic but having the crucial property of 'lack of reflectional symmetry' (a property that, as observed above, can be induced in a rotating fluid through interaction of buoyancy-induced convection and Coriolis forces), then a magnetic field will in general grow from an arbitrarily weak initial level, on a scale L large compared with the scale l_0 of the turbulence. This is one of these remarkable situations in which 'order arises out of chaos', the order being evident in the large-scale magnetic field. It may be appropriate to follow the example of Richardson (1922) by summarizing the situation in rhyme:

Convection and diffusion,
In turb'lence with helicity,
Yields order from confusion
In cosmic electricity!

This totally general principle applies no matter what the physical context may be, whether on the planetary, stellar, galactic or even super-galactic scale. It is this generality that makes the approach described above, which derives from that pioneered by Steenbeck *et al.* (1966), so intensely appealing.

5.6 The back-reaction of Lorentz forces

The exponential growth associated with the dynamo action described above must ultimately be arrested by the action of Lorentz forces which may

have a two-fold effect: (i) the generation of motion on the scale L of the growing field, and (ii) the suppression of the turbulence (or at least severe modification) on the scale l_0 which provides the α-effect. The latter effect is the easier to analyse, since one has as a starting point the Alfvén-wave type of analysis described in § 3 above: the effect of a strong locally uniform magnetic field is to cause the constituent eddies of the turbulence either to propagate as Alfvén waves, or, if resistive damping is strong (as it is when R_m is small), to decay without oscillation.

There are two aspects of the behaviour that are worth noting. First, a locally uniform magnetic field induces strong local anisotropy in the turbulent field, modes with vorticity perpendicular to the magnetic field being most strongly damped. The dynamic effect of the field may be estimated in terms of a (dimensionless) *magnetic interaction parameter* N defined by

$$N = \frac{B_0^2 l_0}{\mu_0 \rho \eta v_0}, \tag{5.34}$$

and becomes strong when the local mean field $\boldsymbol{B}_0$ grows strong so that $N \gg 1$. It has been shown (Moffatt 1967) that under this condition, and provided $NR_m^3 \ll 1$, turbulence that is initially isotropic becomes locally two-dimensional (invariant along the direction of $\boldsymbol{B}_0$), with kinetic energy ultimately equally partitioned between the components (u, v) perpendicular to $\boldsymbol{B}_0$ and the component w parallel to $\boldsymbol{B}_0$, i.e.

$$\langle w^2 \rangle = \langle u^2 \rangle + \langle v^2 \rangle . \tag{5.35}$$

This obviously has implications for the α-effect, which is suppressed in magnitude and which no longer remains isotropic. The effects can be exceedingly complex, and it would be inappropriate to attempt to describe them here; there can be no question however that, if the turbulence is maintained by a prescribed force distribution $\boldsymbol{f}(\boldsymbol{x}, t)$, then the large-scale magnetic field must ultimately saturate at a level determined in principle by the statistics of this forcing (in particular by the mean-square values $\langle \boldsymbol{f}^2 \rangle$ and $\langle \boldsymbol{f} \cdot \nabla \wedge \boldsymbol{f} \rangle$) in conjunction with the relevant physical properties of the fluid, namely ν and η.

The second feature to note is that on scales of order l_0 and smaller, the spectrum $\Gamma(k)$ of field fluctuations $\boldsymbol{b}$ is related to the spectrum $E(k)$ of $\boldsymbol{v}$ in a way that can be derived from the fluctuation equation (5.8). This calculation was first carried out by Golitsin (1960) (see also Moffatt 1961); it shows that if there is an inertial range of wavenumbers in which $E(k) \sim k^{-5/3}$ (see Chapter 5), then in this range, $\Gamma(k) \sim k^{-11/3}$. This is one prediction where theory is now corroborated by experiment: Odier, Pinton & Fauve (1998) found, in experiments on liquid gallium with values of R_m

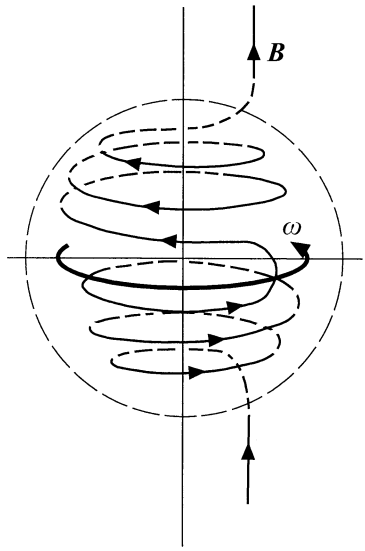

Figure 10. Generation of toroidal fields by differential rotation: the poloidal field is 'gripped' by the flow, and 'cranked' around the axis of symmetry (see, for example, Moffatt 1978).

in the range 1.3 to 15, that $\Gamma(k)$ scales like $k^{-\mu}$, with $\mu = 3.7 \pm 0.2$, neatly embracing the value $11/3 = 3.66$. In a branch of magnetohydrodynamics in which experimental results are sparse, this result stands out, and gives hope that more central aspects of dynamo theory may also soon be subject to experimental investigation and verification.

5.7 The $\alpha\omega$-dynamo

It would be misleading to leave the subject of dynamo theory without mentioning a mechanism of field generation that is just as important as the α-effect in the context of stellar and planetary magnetism, namely the generation of toroidal (or zonal) magnetic field from poloidal (or meridional) field by differential rotation. This mechanism, which operates in an axisymmetric system, is easily understood with reference to figure 10: if the angular velocity $\omega(r, \theta)$ is non-uniform along a field line of the poloidal field $\boldsymbol{B}_P(r, \theta)$, i.e. if $\boldsymbol{B}_P \cdot \nabla\omega \neq 0$, then the field line will be 'cranked' around the axis of symmetry, and a toroidal component $B_T(r, \theta)$ will be generated. This process is ultimately limited by field diffusion; detailed analysis (see, for example, Moffatt 1978) shows that, if $R_{m\omega}$ is a magnetic Reynolds number based on

the strength and scale of the differential rotation, then B_T saturates at a level $O(R_{m\omega})|\boldsymbol{B}_P|$.

This of course is on the assumption that, through some other mechanism, the field $\boldsymbol{B}_P$ is itself maintained at a steady level. There is no axisymmetric mechanism that can achieve this (Cowling 1934), and it is of course here that the α-effect is required. The $\alpha\omega$-dynamo incorporates both effects in the dynamo cycle:

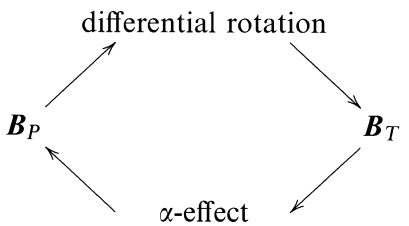

The α-effect here operates through the action of helical convection (i.e. convection influenced by Coriolis forces), which acts on the toroidal field in much the same manner as described in § 5.4 above. The non-axisymmetric character of such a convective process is what allows the $\alpha\omega$-dynamo to escape the strait-jacket of Cowling's theorem.

Many variants of the $\alpha\omega$-dynamo, involving particular distributions of $\alpha(r,\theta)$ and $\omega(r,\theta)$, have been investigated (see particularly Krause & Rädler 1980), and much effort has been applied over the last 25 years to incorporate the difficult back-reaction of Lorentz forces in these models. Many difficulties still remain to be overcome, particularly in the two most prominent spheres of application, the Earth and the Sun. But it seems likely that, in the ultimate theories of the origins of both geomagnetism and heliomagnetism which may be expected to evolve over the next 50 years, both α-effect and ω-effect will survive as essential ingredients.

6 Relaxation to magnetostatic equilibrium

We turn now to a problem that is in some respects the opposite of the dynamo problem. As we have repeatedly observed, the Lorentz force $\boldsymbol{F} = \boldsymbol{j} \wedge \boldsymbol{B}$ is in general rotational and so drives a fluid motion; through this mechanism, magnetic energy can be converted to kinetic energy of motion, and if the fluid is viscous this energy is dissipated into heat. Thus, even if the fluid can be regarded as perfectly conducting (i.e. $\eta = 0$ or $R_m = \infty$) so that Joule dissipation is negligible, there is an alternative indirect route by which magnetic energy may dissipate, and this dissipation mechanism will persist for so long as $\nabla \wedge \boldsymbol{F} \neq 0$.

Insofar as the fluid is perfectly conducting however, the topology of the magnetic field is conserved during this 'relaxation' process; in particular, all links and knots present in the magnetic flux tubes at the initial instant $t = 0$ are present at least for all finite times $t > 0$. It is physically obvious that the magnetic energy cannot decay to zero under such circumstances; the only alternative possibility is that the field relaxes to an equilibrium compatible with its initial topology and for which $\nabla \wedge \boldsymbol{F} = 0$. In such a state

$$\boldsymbol{F} = \boldsymbol{j} \wedge \boldsymbol{B} = \nabla p, \tag{6.1}$$

i.e. the Lorentz force is balanced by a pressure gradient and the fluid is at rest: the field is in magnetostatic equilibrium (see, for example, Biskamp 1993).

We shall look more closely at the details of this process in the following subsections; for the moment it need merely be noted that we are faced here with an intriguing class of problems of variational type: to minimize a positive functional of the field $\boldsymbol{B}$ (here the magnetic energy) subject to conservation of the field topology; this topological constraint is conveniently captured by the requirement that only frozen-field distortions of $\boldsymbol{B}$, i.e. those governed by the frozen-field equation

$$\frac{\partial \boldsymbol{B}}{\partial t} = \nabla \wedge (\boldsymbol{v} \wedge \boldsymbol{B}), \tag{6.2}$$

are to be considered. We know that this equation guarantees conservation of magnetic helicity $\mathscr{H}_M$ (§ 2.2 above); but since (6.2) tells us that the field $\boldsymbol{B}$ in effect deforms with the flow, *all* its topological properties (i.e. those properties that are invariant under continuous deformation) are automatically conserved under this evolution.

We may look at this also from a Lagrangian point of view. Let the Lagrangian particle path associated with the flow $\boldsymbol{v}(\boldsymbol{x}, t)$ be given by

$$\boldsymbol{x} \to \boldsymbol{X}(\boldsymbol{x}, t), \quad \partial \boldsymbol{X}/\partial t = \boldsymbol{v}, \quad \boldsymbol{X}(\boldsymbol{x}, 0) = \boldsymbol{x}. \tag{6.3}$$

Then the Lagrangian statement equivalent to (6.2) is

$$\frac{B_i(\boldsymbol{X})}{\rho(\boldsymbol{X})} = \frac{B_j(\boldsymbol{x})}{\rho(\boldsymbol{x})} \frac{\partial X_i}{\partial x_j}, \tag{6.4}$$

where ρ is the density field. The deformation tensor $\partial X_i/\partial x_j$ encapsulates both the rotation and stretching of the field element of $\boldsymbol{B}$ as it is transported from $\boldsymbol{x}$ to $\boldsymbol{X}$ in time t. If the fluid is incompressible, then of course $\rho(\boldsymbol{X}) = \rho(\boldsymbol{x})$. Note that (6.3) is a family of mappings continuously dependent on the parameter t, and being the identity mapping at $t = 0$; in the language of topology, it is an 'isotopy'.

6.1 The structure of magnetostatic equilibrium states

Equation (6.1) places a strong constraint on the structure of possible magnetostatic equilibria; it implies that

$$\boldsymbol{j}\cdot\nabla p = 0 \qquad \text{and} \qquad \boldsymbol{B}\cdot\nabla p = 0, \tag{6.5}$$

so that, in any region where $\nabla p \neq 0$, both the current lines ($\boldsymbol{j}$-lines) and field lines ($\boldsymbol{B}$-lines) must lie on surfaces $p = \text{const}$.

In any region where $\nabla p \equiv 0$, it follows from (6.1) that $\boldsymbol{j}$ is parallel to $\boldsymbol{B}$, i.e.

$$\boldsymbol{j} = \gamma(\boldsymbol{x})\boldsymbol{B} \tag{6.6}$$

for some scalar field $\gamma(\boldsymbol{x})$. The field $\boldsymbol{B}$ is then described as 'force-free' in this region. There is a considerable literature devoted to the subject of force-free fields (see particularly Marsh 1996); here we simply note that, on taking the divergence of (6.6) and using $\nabla\cdot\boldsymbol{j} = \nabla\cdot\boldsymbol{B} = 0$, we obtain

$$\boldsymbol{B}\cdot\nabla\gamma = 0, \tag{6.7}$$

so that now the $\boldsymbol{B}$-lines lie on surfaces $\gamma = \text{const}$. The only possible escape from this (topological) constraint is when $\nabla\gamma \equiv 0$ and $\gamma = \text{const}$. The field $\boldsymbol{B}$ is then a 'Beltrami' field. We have seen one example in (5.25) above; a more general field satisfying $\nabla\wedge\boldsymbol{B} = \gamma\boldsymbol{B}$ may be constructed as a superposition of circularly polarized Fourier modes in the form

$$\boldsymbol{B}(\boldsymbol{x}) = \int_{|\boldsymbol{k}|=\gamma} \left(\hat{\boldsymbol{b}}(\boldsymbol{k}) + \mathrm{i}\hat{\boldsymbol{k}}\wedge\hat{\boldsymbol{b}}(\boldsymbol{k})\right) \mathrm{e}^{\mathrm{i}\boldsymbol{k}\cdot\boldsymbol{x}}, \tag{6.8}$$

where $\hat{\boldsymbol{k}} = \boldsymbol{k}/|\boldsymbol{k}|$ and $\boldsymbol{k}\cdot\hat{\boldsymbol{b}}(\boldsymbol{k}) = 0$. With such a field, the $\boldsymbol{B}$-lines are no longer constrained to lie on surfaces; the particular field (5.25) exhibits the property of chaotic wandering of $\boldsymbol{B}$-lines (Hénon 1966; Arnold 1966; Dombre *et al.* 1986), and it may be conjectured that this is a generic property of force-free fields of the general form (6.8).

6.2 Magnetic relaxation

Suppose now that incompressible fluid is contained in a domain $\mathscr{D}$ with fixed rigid boundary $\partial\mathscr{D}$. For the reasons already indicated, let us suppose that this fluid is viscous and perfectly conducting. Such a combination of fluid properties is physically artificial; but no matter – this is a situation where the end justifies the means! We suppose that at $t = 0$ the fluid is at rest and that it supports a magnetic field $\boldsymbol{B}_0(\boldsymbol{x})$ where $\boldsymbol{n}\cdot\boldsymbol{B}_0 = 0$ on $\partial\mathscr{D}$. Clearly this condition of tangency of the field at the surface $\partial\mathscr{D}$ persists under the

subsequent evolution. This evolution is governed by equation (6.2) together with (3.3), or equivalently

$$\left(\frac{\partial \boldsymbol{v}}{\partial t} + \boldsymbol{v}\cdot\nabla\boldsymbol{v}\right) = -\frac{1}{\rho}\nabla p + \frac{1}{\rho}\boldsymbol{j}\wedge\boldsymbol{B} + \nu\nabla^2\boldsymbol{v}\,. \tag{6.9}$$

The velocity $\boldsymbol{v}$ satisfies the no-slip condition $\boldsymbol{v} = 0$ on $\partial\mathscr{D}$.

From (6.2) and (6.9) we may easily construct an energy equation. Let

$$M(t) = \tfrac{1}{2}\mu_0\int_{\mathscr{D}} \boldsymbol{B}^2\,\mathrm{d}V \qquad \text{and} \qquad K(t) = \tfrac{1}{2}\rho\int_{\mathscr{D}} \boldsymbol{v}^2\,\mathrm{d}V\,, \tag{6.10}$$

the magnetic and kinetic energies. Then this energy equation is

$$\frac{\mathrm{d}}{\mathrm{d}t}(M+K) = -\rho\nu\int \boldsymbol{\omega}^2\,\mathrm{d}V\,, \tag{6.11}$$

where $\boldsymbol{\omega} = \nabla\wedge\boldsymbol{v}$. As expected, the sole mechanism of dissipation is viscosity.

Now let us suppose that the topology of the initial field $\boldsymbol{B}_0(\boldsymbol{x})$ is non-trivial, and in particular, that its helicity $\mathscr{H}_M$ is non-zero. This helicity is conserved under (6.2); moreover non-zero helicity clearly implies a positive lower bound for magnetic energy (Arnold 1974):

$$M \geqslant L_{\mathscr{D}}^{-1}|\mathscr{H}_M|\,, \tag{6.12}$$

where $L_{\mathscr{D}}$ is a constant with the dimensions of length; this constant is determined by the geometry of $\mathscr{D}$ and can normally be interpreted as a representative linear scale of $\mathscr{D}$.

Since $M+K$ is monotonic decreasing (by (6.11)) and bounded below (by (6.12)), it must tend to a positive constant; hence the right-hand side of (6.11) tends to zero as $t\to\infty$. Provided no singularity of $\boldsymbol{\omega}$ develops, it follows that $\boldsymbol{\omega}\to 0$ for all $\boldsymbol{x}\in\mathscr{D}$ as $t\to\infty$; it is then not difficult to show that, under the no-slip condition on $\partial\mathscr{D}$, $\boldsymbol{v}\to 0$ also for all $\boldsymbol{x}\in\mathscr{D}$, i.e. the limit state is indeed magnetostatic. Thus, as $t\to\infty$, $\boldsymbol{B}\to\boldsymbol{B}^E(\boldsymbol{x})$, $\boldsymbol{j}\to\boldsymbol{j}^E(\boldsymbol{x})$, where

$$\boldsymbol{j}^E\wedge\boldsymbol{B}^E = \nabla p^E\,. \tag{6.13}$$

This evolutionary process may be represented pictorially by a 'trajectory' $\mathscr{J}$ in the function space $\mathscr{F}$ of solenoidal vector fields of finite energy (figure 11). This trajectory is confined to a subspace $\mathscr{S}$ of those fields that can be obtained from $\boldsymbol{B}_0(\boldsymbol{x})$ by isotopic (frozen-field) deformation. Such a subspace, described as 'isomagnetic' is indicated as a surface in figure 11, but this is a misleading simplification, since it is in fact infinite-dimensional. Nevertheless, $\mathscr{F}$ may be thought of as 'foliated' by such isomagnetic subspaces, the fields on any such subspace being 'topologically accessible' one from another by isotopic deformation. This concept of an 'isomagnetic subspace' is closely

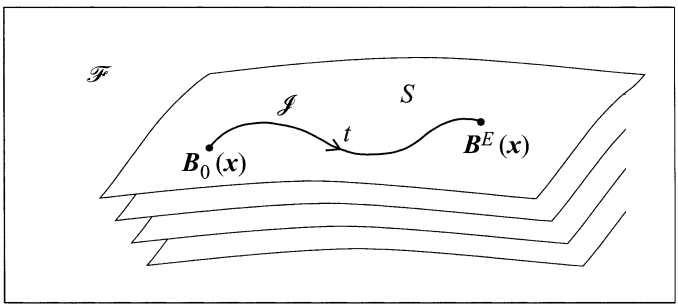

Figure 11. Schematic representation of the process of magnetic relaxation. This is represented by the trajectory $\mathscr{J}$ on the 'isomagnetic' folium S in the function space $\mathscr{F}$ of solenoidal fields $\boldsymbol{B}(\boldsymbol{x})$ of finite energy; the stacked sheets represent the isomagnetic foliation of this space (Moffatt 1985*a*).

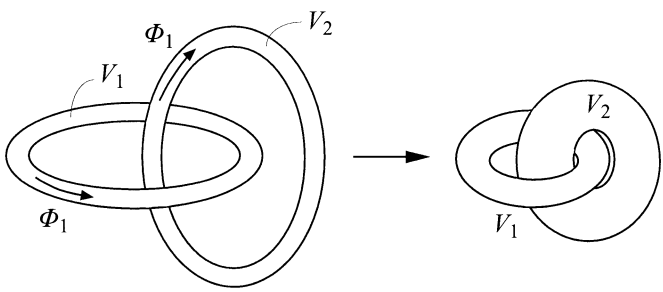

Figure 12. Relaxation of linked flux tubes due to Maxwell tension along the axes of the tubes; a tangential discontinuity of field develops when the tubes make contact (Moffatt 1985*a*).

allied to the concept of 'isovorticity' that arises in consideration of the Euler equation of ideal fluid flow (see Chapter 11).

The limit field $\boldsymbol{B}^E(\boldsymbol{x})$ is itself topologically accessible from the initial field $\boldsymbol{B}_0(\boldsymbol{x})$. Note however that the mapping (6.3) may develop discontinuities in the limit $t \to \infty$, so we cannot make the stronger assertion that $\boldsymbol{B}^E(\boldsymbol{x})$ is 'topologically equivalent' to $\boldsymbol{B}_0(\boldsymbol{x})$. The reason for the possible development of discontinuities should be apparent from consideration of the situation depicted in figure 12. Here the field $\boldsymbol{B}_0(\boldsymbol{x})$ is supposed confined to two linked flux tubes of volumes V_1, V_2 and carrying axial fluxes Φ_1, Φ_2 respectively. The domain $\mathscr{D}$ may be taken as the space $\mathbb{R}^3$. The Lorentz force is equivalent to a 'Maxwell tension' in the lines of force which causes contraction of both tubes (the magnetic pressure gradient across the tubes is compensated by an adjustment of fluid pressure, the fluid being assumed incompressible). Tube contraction is accompanied by increase of tube cross-section, both V_1 and

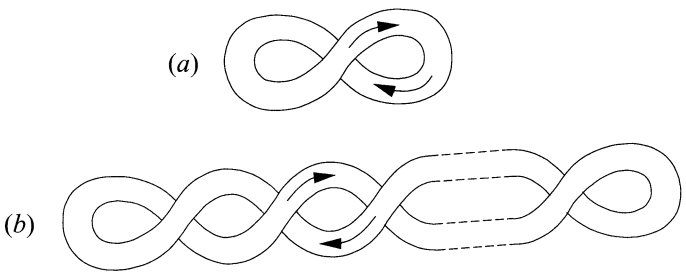

Figure 13. (*a*) Single flux tube with axial flux Φ and uniform internal twist h; the helicity is $\pm h\Phi^2$. (*b*) Multiply kinked tube, believed to be the preferred configuration when $h \gg 1$; the internal 'twist' is converted to 'writhe' which may be estimated by the number of crossings.

V_2 being conserved. Thus contact of the two tubes is inevitable in the limit $t \to \infty$, this contact being achieved by a 'squeeze-film' mechanism in which the (viscous) fluid is squeezed from the space between the two tubes as these contract towards contiguity.

Note that the fluxes Φ_1 and Φ_2, and also naturally the helicity $\mathscr{H}_M = 2\Phi_1\Phi_2$, are conserved during the relaxation process.

6.3 Relaxation of a single flux tube

The case of a single, possibly knotted, flux tube is of special interest. This is an aspect of the general theory whose peculiar interest was anticipated by Kelvin in his seminal paper of 1869 – although there Kelvin was concerned with vortex tubes rather than magnetic flux tubes; the latter are in fact more amenable to detailed investigation.

Consider first the case of an unknotted flux tube (figure 13*a*) carrying axial flux Φ. Suppose further that the field within the tube is twisted in such a way that any pair of field lines has linking number h; such a pair may be considered as the boundaries of a 'ribbon' which is twisted through an angle $2\pi h$ before being joined end-to-end. The helicity associated with the field distribution (Berger & Field 1984) is then given by

$$\mathscr{H}_M = \pm h\Phi^2, \tag{6.14}$$

where the + or − is chosen according to whether the twist is right-handed or left-handed. The description may be generalized in an obvious way to non-integer values of h; if h is irrational, then the field lines are not closed curves, but cover a family of nested toruses.

If $h = 0$, then there is no topological constraint to contraction of the

field lines and reduction of magnetic energy: each field line can, in principle, contract to a point (as $t \to \infty$) and it therefore seems inevitable that the unique limit state that minimizes M (at $M = 0$) is $\boldsymbol{B}^E(\boldsymbol{x}) \equiv 0$.

If $h \neq 0$, then M is constrained by (6.12), and, on dimensional grounds, the minimum value of M, M^E say, is given by

$$M^E = m(h)\Phi^2 V^{-1/3}, \tag{6.15}$$

where V is the volume of the flux tube, and $m(h)$ is a dimensionless function of the dimensionless number h. The form of this function may be easily estimated as follows (Chui & Moffatt 1995): the axial field B_T in the tube is proportional to the tube length L, so that the corresponding contribution to magnetic energy M_T scales like $\Phi^2 L^2/V$. The transverse field B_P due to twist in the tube is proportional to $hV^{1/2}L^{-3/2}B_T$, and the additional contribution M_P therefore scales like $h^2\Phi^2/L$. Clearly to minimize $M = M_T + M_P$, L adjusts itself so that the two contributions are of the same order of magnitude, i.e.

$$L \sim h^{2/3}V^{1/3} \tag{6.16}$$

and then $M \sim h^{4/3}\Phi^2 V^{-1/3}$; thus

$$m(h) \sim h^{4/3} \tag{6.17}$$

where the symbol $\sim$ is used to mean 'scales like'.

Note that, if $h \gg 1$, then from (6.16), the tube cross-section $A = V/L \sim h^{-2/3}V^{2/3}$, and is small; this results from contraction of the cross-sectional field B_P (in the above notation). Simple estimates suggest that the tube is subject to 'kink instabilities' in this limit, the limit state of minimum energy being multiply kinked as indicated in figure 13(*b*). The associated conversion of 'twist' to 'writhe' (the sum being precisely the conserved h), is discussed by Moffatt & Ricca (1992).

Consider now a flux tube knotted in the form of an arbitrary knot K. Again we may suppose that the field structure within the tube is one of 'uniform twist', in which each pair of $\boldsymbol{B}$-lines has the same linking number h. That this number is arbitrary should be evident from the fact that, through cutting, twisting and reconnecting the tube, it may be changed by an arbitrary amount. This freedom to specify h is what knot-theorists describe as 'framing', and the particular choice of twist that gives $h = 0$ is described as 'zero-framing'. In any event, the helicity of the framed magnetic flux tube is still given by $\mathscr{H}_M = h\Phi^2$ (since it is just the pairwise linkages that contribute to $\mathscr{H}_M$, as for an unknotted tube).

As regards the minimum-energy state of such a tube, the argument leading

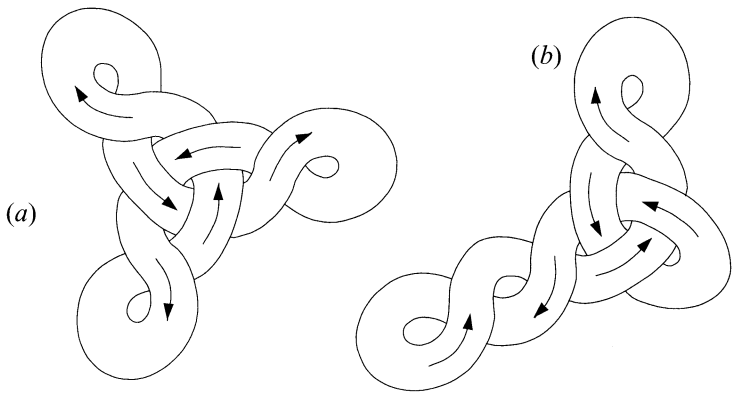

Figure 14. Conjectured minimum-energy configuration for the trefoil knot for the same value of h (count the crossings!).

to (6.15) still applies (Moffatt 1990), but now the function $m(h)$ may depend on the knot K as well as on h. We therefore write it as $m_K(h)$, a real-valued function which is a 'property' of the knot K. The argument leading to (6.17) is now valid only for large h (since for $h = O(1)$ there is now a topological barrier to unlimited decrease of knot length L); thus we have

$$m_K(h) \sim h^{4/3} \qquad \text{for} \qquad h \gg 1. \tag{6.18}$$

Note also that there may be more than one minimum-energy state: two possibilities for the trefoil knot with $h = 6$ are indicated in figure 14.

6.4 Ideal knots

There is a connection, as yet not fully understood, between the foregoing description of minimum-energy knotted flux tubes and the concept of 'ideal knots' (Stasiak, Katritch & Kauffman 1998). Consider a closed curve C in the form of a knot K; we may obviously deform C continuously without changing K. Let us fix the length L of C, and construct a tube around C of circular cross-section radius r centred on C. The volume of this tube is $V = \pi r^2 L$. Let us now gradually increase r until either the tube makes contact with itself or until r equals the minimum radius of curvature on C; the volume is then $V = V_m(C)$ say. We may now ask: what form does the curve C take (for given K and L) so that $V_m(C)$ is maximized? In this configuration, in Stasiak *et al.*'s terminology, the knot is 'ideal'.

Since maximizing V for fixed L is equivalent to minimizing L for fixed V, the above construction of an ideal knot is closely related to the process

of magnetic relaxation to a minimum-energy state, at least when the twist parameter h is small. The concept of *twist*, or equivalently framing, plays no part in Stasiak *et al.*'s construction. The connection between the constructions, one purely geometrical in character, the other of more physical origin, is intriguing and deserves further study. There is some evidence, presented by Stasiak *et al.* (1996), that knotted DNA strands have a tendency to seek the ideal configuration appropriate to the knot. The reason for this sort of behaviour may well be found within a 'minimum-energy' formulation of the problem. Much remains to be done in this new and challenging field.

6.5 A paradox and its resolution

The argument of § 6.2 contains an altogether astonishing implication: for a given magnetic field $\boldsymbol{B}_0(\boldsymbol{x})$ of arbitrary topology, there exists a magnetostatic equilibrium field $\boldsymbol{B}^E(\boldsymbol{x})$ that is topologically accessible from $\boldsymbol{B}_0(\boldsymbol{x})$ – this accessibility being realized by the magnetic relaxation process.

Now the general three-dimensional field $\boldsymbol{B}_0(\boldsymbol{x})$ in a finite domain $\mathscr{D}$ is likely to be chaotic, i.e. the $\boldsymbol{B}_0$-lines are generally not closed and do not lie on surfaces. This is because the three-dimensional nonlinear dynamical system

$$\mathrm{d}\boldsymbol{x}/\mathrm{d}t = \boldsymbol{B}_0(\boldsymbol{x}) \tag{6.19}$$

is in general non-integrable. An example of the resulting chaotic behaviour may be found in Bajer & Moffatt (1990), in which the Cartesian components of $\boldsymbol{B}_0(\boldsymbol{x})$ are taken to be quadratic functions of the coordinates (x, y, z).

A field that is chaotic cannot relax to one whose field lines lie on surfaces; hence, in general, the relaxed field $\boldsymbol{B}^E(\boldsymbol{x})$ must also be chaotic. But we have seen in § 6.1 that in this case

$$\nabla \wedge \boldsymbol{B}^E = \gamma \mu_0 \boldsymbol{B}^E \tag{6.20}$$

with γ constant, i.e. at least within the region in which $\boldsymbol{B}^E$ is chaotic, it is also a Beltrami field. As first pointed out by Arnold (1974), if we confine attention to analytic fields, the family of solutions of (6.20) is not nearly wide enough to include all possible topologies (and all possible degrees of chaos) in the relaxed field $\boldsymbol{B}^E$; and yet we must allow for all possible topologies, since the topology of $\boldsymbol{B}_0(\boldsymbol{x})$ was arbitrary.

How then is this contradiction to be resolved? Partly, no doubt, through accepting that, as indicated by the example of figure 12, tangential discontinuities of $\boldsymbol{B}$ (i.e. current sheets) will appear quite naturally in the course of relaxation, i.e. there is no reason to believe that the relaxed field $\boldsymbol{B}^E$ will

be analytic, even if $\boldsymbol{B}_0$ is analytic. Second, and more subtly, it is known that there are always 'islands of regularity' within any sea of chaos; during relaxation, the boundaries of such islands can become infinitely deformed so that the region of chaos within which the field $\boldsymbol{B}^E$ satisfies (6.20) may exhibit an arbitrarily complex geometry; the simplicity of (6.20) is gained at the cost of geometrical complexity of the region within which it is valid.

Magnetic relaxation is a process that can in principle be realized numerically; however, no satisfactory way has yet been found to provide accurate simulation in three dimensions of the frozen-field equation (6.2). Field relaxation in two dimensions *has* been accomplished by Linardatos (1993), who shows a clear tendency for current sheets to form due to collapse of the separatrices passing through saddle points of the field; but the problem of chaos does not arise for two-dimensional fields.

We note that the formation of current sheets, which may be recognized as a natural concomitant of magnetic relaxation to a minimum-energy state, is of absolutely central importance in solar physics: it is a prime mechanism for the explosive activity associated with solar flares and for consequential heating of the solar corona (Parker 1994). Whereas dynamo theory is central to an understanding of the internal origins of solar magnetism, magnetic relaxation provides the key to a proper understanding of observed external magnetic activity. The two process, both fundamental, are complementary in more senses than one (Parker 1979; see also Priest 1982).

7 Concluding remarks

In this essay, I have attempted to convey the flavour, rather than the detail, of three overlapping areas of magnetohydrodynamics in which I have been successively involved over the last 40 years. In 1960, the subject was relatively young and it attracted a huge cohort of researchers, active particularly in the contexts of astrophysics and fusion (plasma) physics. Great progress was made, notably in dynamo theory in the 1960s, the 1970s being more a period of consolidation. In more recent years, as in other branches of fluid mechanics, the computer has played an increasingly important role in allowing the investigation of nonlinear effects frequently beyond the reach of analytical study. Some fascinating new areas have emerged, most notably the area treated in §6 above in which the global topology of the magnetic field plays a central role. It may be noted that there is an exact analogy between the magnetostatic equation (6.13) and the steady Euler equation of ideal hydrodynamics, so that the magnetic relaxation technique provides an indirect means of determining solutions of the steady Euler equations

of arbitrary streamline topology (Moffatt 1985*a*). There is a rich interplay between MHD and 'ordinary' fluid dynamics that stems from this analogy, in subtle conjunction with the (different) analogy between (2.4) and (2.6). Magnetohydrodynamics is a richly rewarding field of study, not only in its own right, but also through the illumination of more classical areas of fluid dynamics that this interplay provides.

References

ALFVÉN, H. 1950 *Cosmical Electrodynamics.* Oxford University Press.

ARNOLD, V. I. 1966 Sur la topologie des écoulements stationnaires des fluides parfaits. *C. R. Acad. Sci. Paris* **261**, 17–20.

ARNOLD, V. I. 1974 The asymptotic Hopf invariant and its applications. In *Proc. Summer School in Differential Equations, Erevan 1974.* Armenian SSR Acad. Sci. [English transl: *Sel. Math. Sov.* **5** (1986), 327–345].

ARNOLD, V. I. & KHESIN, B. A. 1998 *Topological Methods in Hydrodynamics.* Springer.

BAJER, K. & MOFFATT, H. K. 1990 On a class of steady confined Stokes flows with chaotic streamlines. *J. Fluid Mech.* **212**, 337–363.

BATCHELOR, G. K. 1950 On the spontaneous magnetic field in a conducting liquid in turbulent motion. *Proc. R. Soc. Lond.* A **201**, 405–416.

BERGER, M. A. & FIELD, G. B. 1984 The topological properties of magnetic helicity. *J. Fluid Mech.* **147**, 133–148.

BISKAMP, D. 1993 *Nonlinear Magnetohydrodynamics.* Cambridge University Press.

BOJAREVIČS, V., FREIBERGS, YA., SHILOVA, E. I. & SHCHERBININ, E. V. 1989 *Electrically Induced Vortical Flows.* Kluwer.

BRAGINSKII, S. I. 1964 Theory of the hydromagnetic dynamo. *Sov. Phys. JETP* **20**, 1462–1471.

BRAUNBEK, W. 1932 Eine neue Methode electrodenloser Leitfähigkeitsmessung. *Z. Phys.* **73**, 312–334.

CHANDRASEKHAR, S. 1961 *Hydrodynamic and Hydromagnetic Stability.* Clarendon.

CHILDRESS, S. & GILBERT, A. D. 1995 *Stretch, Twist, Fold: the Fast Dynamo.* Springer.

CHUI, A. Y. K. & MOFFATT, H. K. 1995 The energy and helicity of knotted magnetic flux tubes. *Proc. R. Soc. Lond.* A **451**, 609–629.

COOK, A. H. 1980 *Interiors of the Planets.* Cambridge University Press.

COWLING, T. G. 1934 The magnetic field of sunspots. *Mon. Not. R. AstrON. Soc.* **94**, 39–48.

COWLING, T. G. 1957 *Magnetohydrodynamics.* Interscience; 2nd Edn 1975, Adam Hilger Ltd., Bristol.

DOMBRE, T., FRISCH, U., GREENE, J. M., HÉNON, M., MEHR, A. & SOWARD, A. M. 1986 Chaotic streamlines in the ABC flows. *J. Fluid Mech.* **167**, 353–391.

DAVIDSON, P. A., KINNEAR, D., LINGWOOD, R. J., SHORT, D. J. & HE, X. 1999 The role of Ekman pumping and the dominance of swirl in confined flow driven by Lorentz forces. *Eur. J. Mech.* B/*Fluids* **18**, 693–711.

GOLITSIN, G. 1960 Fluctuations of magnetic field and current density in turbulent flows of weakly conducting fluids. *Sov. Phys. Dokl.* **132**, 315–318.

HÉNON, M. 1966 Sur la topologie des lignes de courant dans un cas particulier. *C. R. Acad. Sci. Paris* A **262**, 312–314.

JACOBS, J. A. 1984 *Reversals of the Earth's Magnetic Field.* Adam Hilger Ltd., Bristol.

KELVIN, LORD (then W. THOMSON) 1869 On vortex motion. *Trans. R. Soc. Edin.*, **25**, 217–260.

KRAUSE, F. & RÄDLER, K.-H. 1980 *Magnetohydrodynamics and Dynamo Theory.* Pergamon.

LINARDATOS, D. 1993 Determination of two-dimensional magnetostatic equilibria and analogous Euler flows. *J. Fluid Mech.* **246**, 569–591.

MARSH, G. E. 1996 *Force-free Magnetic Fields: Solutions, Topology and Applications.* World Scientific.

MESTEL, A. J. 1982 Magnetic levitation of liquid metals. *J. Fluid Mech.* **117**, 27–43.

MOFFATT, H. K. 1961 The amplification of a weak applied magnetic field by turbulence in fluids of moderate conductivity. *J. Fluid Mech.* **11**, 625–635.

MOFFATT, H. K. 1965 On fluid flow induced by a rotating magnetic field. *J. Fluid Mech.* **22**, 521–528

MOFFATT, H. K. 1967 On the suppression of turbulence by a uniform magnetic field. *J. Fluid Mech.* **28**, 571–592.

MOFFATT, H. K. 1969 The degree of knottedness of tangled vortex lines. *J. Fluid Mech.* **35**, 117–129.

MOFFATT, H. K. 1978 *Magnetic Field Generation in Electrically Conducting Fluids.* Cambridge University Press.

MOFFATT, H. K. 1985*a* Magnetostatic equilibria and analogous Euler flows of arbitrarily complex topology. Part 1. Fundamentals. *J. Fluid Mech.* **159**, 359–378.

MOFFATT, H. K. 1985*b* High frequency excitation of liquid metal systems. In *Metallurgical Applications of Magnetohydrodynamics* (ed. H. K. Moffatt & M. R. E. Proctor), pp. 180–189. Metals Society, London.

MOFFATT, H. K. & PROCTOR, M. R. E. (Eds.) 1984 *Metallurgical Applications of Magnetohydrodynamics.* Metals Society, London.

MOFFATT, H. K. 1990 The energy spectrum of knots and links. *Nature* **347**, 367–369.

MOFFATT, H. K. & RICCA, R. L. 1992 Helicity and the Călugăreanu invariant. *Proc. R. Soc. Lond.* A **439**, 411–429.

MOREAU, R. 1990 *Magnetohydrodynamics.* Kluwer.

NORTHRUP, E. F. 1907 Some newly observed manifestations of forces in the interior of an electric conductor. *Phys. Rev.* **24**, 474–497.

ODIER, P., PINTON, J.-F. & FAUVE, S. 1998 Advection of a magnetic field by a turbulent swirling flow. *Phys. Rev.* E **58**, 7397–7401.

PARKER, E. N. 1955 Hydromagnetic dynamo models. *Astrophys. J.* **122**, 293–314.

PARKER, E. N. 1979 *Cosmical Magnetic Fields.* Clarendon.

PARKER, E. N. 1994 *Spontaneous Current Sheets in Magnetic Fields.* Oxford University Press.

PRIEST, E. R. 1982 *Solar Magnetohydrodynamics.* D. Reidel.

RICHARDSON, L. F. 1922 *Weather Prediction by Numerical Process.* Cambridge University Press.

SCHUSTER, A. 1912 A critical examination of the possible causes of terrestrial magnetism. *Proc. Phys. Soc. Lond.* **24**, 121–137.

SNEYD, A. D. & MOFFATT, H. K. 1982 Fluid-dynamical aspects of the levitation melting process. *J. Fluid Mech.* **117**, 45–70.

STASIAK, A., KATRITCH, V., BEDNAR, J., MICHOUD, D. & DUBOCHET, J. 1996 Electrophoretic mobility of DNA knots. *Nature* **384**, 122.

STASIAK, A., KATRITCH, V. & KAUFFMAN, L. H. 1998 *Ideal Knots.* World Scientific.

STEENBECK, M., KRAUSE, F. & RÄDLER, K.-H. 1966 Berechnung der mittleren

Lorentz-Feldstärke für ein elektrisch leitendes Medium in turbulenter, durch Coriolis-Kräfte beeinfluster Bewegung. *Z. Naturforsch.* **21a**, 369–376.

VAINSHTEIN, S. I. & ZELDOVICH, YA. B. 1972 Origin of magnetic fields in astrophysics. *Sov. Phys. Usp.* **15**, 159–172.

WOLTJER, L. 1958 A theorem on force-free magnetic fields. *Proc. Natl Acad. Sci.* **44**, 489–491.

ZELDOVICH, YA. B., RUZMAIKIN, A. A. & SOKOLOFF, D. D. 1983 *Magnetic Fields in Astrophysics.* Gordon and Breach.

Isaac Newton Institute for Mathematical Sciences, University of Cambridge, 20 Clarkson Road, Cambridge CB3 0EH, UK